Tectonics

RESEARCH ARTICLE
10.1029/2022TC007522

The Montello Thrust and the Active Mountain Front of the Eastern Southern Alps (Northeast Italy)

Vincenzo Picotti[1], Maria Adelaide Romano[2], Alessio Ponza[3], Francesco Luigi Guido[3], and Laura Peruzza[2]

[1]Department of Earth Sciences, ETH Zürich, Zürich, Switzerland, [2]Istituto Nazionale di Oceanografia e di Geofisica Sperimentale OGS – Borgo Grotta Gigante, Sgonico, Italy, [3]Geophi Srl, Bologna, Italy

Key Points:

- The Montello thrust (MT) formed in the late Miocene as splay of the Bassano-Valdobbiadene (BV) thrust. Both account for the active shortening at the front of the Southern Alps
- Based on growing relationships and dated geomorphic features, the MT deformation rates are lower than presently proposed in the literature
- The MT is presently creeping, and is considered as a unique thrust system with the BV thrust, for the understanding of the seismic risks

Correspondence to:
V. Picotti,
vincenzo.picotti@erdw.ethz.ch

Citation:
Picotti, V., Romano, M. A., Ponza, A., Guido, F. L., & Peruzza, L. (2022). The Montello thrust and the active mountain front of the eastern Southern Alps (northeast Italy). *Tectonics*, *41*, e2022TC007522. https://doi.org/10.1029/2022TC007522

Received 10 AUG 2022
Accepted 8 DEC 2022

Author Contributions:
Conceptualization: Vincenzo Picotti, Maria Adelaide Romano, Alessio Ponza, Francesco Luigi Guido, Laura Peruzza
Data curation: Maria Adelaide Romano, Alessio Ponza, Francesco Luigi Guido, Laura Peruzza
Formal analysis: Laura Peruzza
Investigation: Vincenzo Picotti, Maria Adelaide Romano, Alessio Ponza, Francesco Luigi Guido, Laura Peruzza
Methodology: Vincenzo Picotti, Maria Adelaide Romano, Alessio Ponza, Francesco Luigi Guido, Laura Peruzza
Project Administration: Vincenzo Picotti
Software: Maria Adelaide Romano, Alessio Ponza

Abstract New field and subsurface data are combined to define the geometry and evolution of the mountain front of the eastern Southern Alps. The Montello thrust (MT), the southernmost frontal structure, is reconstructed by recently published well-located microseismicity and is connected at depth with the larger Bassano-Valdobbiadene (BV) thrust. The latter started at 10–9 Ma, whereas the MT evolved at 8–6 Ma, as documented by growing unconformities in the foreland deposits and the nature of the natural gas in the anticline culmination. The latter, named Montello anticline, is growing from the upper Miocene to the Quaternary, as shown by surfaces of abrasion and deposition, including the Biadene windgap. The folded bottom of the windgap is a fan unit recently dated to the MIS 3. The MT is presently creeping and its deformation rates are much lower than previous estimates. Most of the late Miocene to Pleistocene deformation at the front of the eastern Southern Alps is accounted for the BV thrust. The reconstructed average shortening rates are in agreement with the geodetic velocity field from literature. The BV and MT are a unique active thrust system with variable slipping and locked patches, whose interactions should be further studied.

Plain Language Summary The definition of the hazard in a seismically active area, such as the front of a mountain chain, requires a precise reconstruction of the geometry of the tectonic structures. In the densely populated foothills of the eastern Southern Alps of Italy, these structures do not reach the surface and are difficult to study. Combining surface and subsurface data with precisely located microseismicity, we provide a synthetic view on the geometry and evolution of the active mountain front. We find that the frontal structure is larger and deeper than previously thought, and it reaches the outskirts of one of the main cities of the area, Treviso. The tectonic stratigraphy of the area, and the geomorphology of a gentle fold (Montello anticline), reveal that the structure (Montello thrust [MT]) is much older, therefore its rates of deformation much lower, than previously thought. Most of the active deformation is focused in a northern structure, named Bassano-Valdobbiadene thrust. Together, these structures account for the Adria-Europe convergence, as defined by geodetic velocity field. Their behavior as thrust system is complex, with locked patches and freely slipping portions, such as the MT and would require a future modeling of their interactions.

1. Introduction

The mountain front of the eastern Southern Alps is a prominent morphological feature that received attention since the end of the XIX century, when Sacco (1898) published the first geological sketch map documenting the Villafranchian (continental Upper Pliocene to Lower Pleistocene) age of the youngest deformed deposits around the Montello hill (Figure 1). The mountain front consists of a large frontal anticline with a steeply tilted southern limb, laterally extended for about 70 km from the west of Bassano to Serravalle (Vittorio Veneto) (Figure 1). Associated to this structure, the Montello hill represents a gentle brachianticline, commonly interpreted as fault-cored (e.g., Benedetti et al., 2000; Schönborn, 1999), forming an around 20 km wide low relief cut by the Nervesa watergap (Piave river) and the Biadene paleovalley (windgap) (Figure 1). The growth of this mountain front was interacting with the erosion operated by the carving of fluvial valleys, only rarely reached by glacier terminations (e.g., Penck & Brückner, 1909; Venzo et al., 1977). The rivers developed in their present valleys during the Tortonian and Messinian, following the establishment of the mountain front, with limited integration of the catchment toward the north (e.g., Massari et al., 1993; Monegato et al., 2010; Stefani et al., 2007).

The geology of the mountain front near the Piave valley and the Montello hill was well documented by Venzo et al. (1977) with detailed maps and cross-sections. Afterward, several authors dealt with the structural setting

Supervision: Vincenzo Picotti, Laura Peruzza
Validation: Vincenzo Picotti, Maria Adelaide Romano, Francesco Luigi Guido, Laura Peruzza
Visualization: Maria Adelaide Romano, Alessio Ponza
Writing – original draft: Vincenzo Picotti, Maria Adelaide Romano, Alessio Ponza, Francesco Luigi Guido, Laura Peruzza
Writing – review & editing: Vincenzo Picotti, Maria Adelaide Romano, Laura Peruzza

of the whole mountain range, with retrodeformable cross-sections (Castellarin et al., 1998; Doglioni, 1992; Schönborn, 1999). All of these previous tectonic interpretations proposed the Montello as branch fault, kinematically linked to the Bassano-Valdobbiadene (BV) thrust, the prominent structure forming the mountain front from Bassano to Serravalle (Figure 1). The first authors proposing the Montello as a separate thrust plane were Galadini et al. (2005).

The stratigraphy of the Montello anticline (MoA) and adjacent foreland was analyzed by several authors, aiming to document the sedimentary record of the tectonic events at the mountain front (e.g., Caputo et al., 2010; Fantoni et al., 2002; Mancin et al., 2009; Massari et al., 1986, 1993).

After the strong seismic events in the Friuli area, east of the Montello hill, in 1976, the eastern southalpine mountain front was explored from a seismotectonic point of view and the seismic sources defined, based on the available geological constraints (e.g., Burrato et al., 2008; Galadini et al., 2005; Peruzza, Poli, et al., 2002; Peruzza, Romano, et al., 2002). Several scholars analyzed its geodetic deformation in order to assess the seismogenic potential of the Montello structure (e.g., Barba et al., 2013; Cheloni et al., 2014; D'Agostino et al., 2005; Danesi et al., 2015; Serpelloni et al., 2016). All of them agree on the occurrence of active shortening across the Montello thrust (MT). Recently, Anderlini et al. (2020), modeling the geodetic deformation at the mountain front, suggested most of the shortening is accounted by the BV thrust, rather than the MT. Therefore, the seismogenic potential of the Montello structure still open to discussion, mainly due to the different shortening rates proposed in the literature (e.g., Benedetti et al., 2000; Galadini et al., 2005; Schönborn, 1999).

In this paper, we intend to reconsider the geology of the Montello area, thanks to the access to a new set of data, including industrial seismic profiles, reservoirs, and wells data. Further data include recently relocated microseismicity (Romano et al., 2019), acquired through a local seismic network deployed around the Collalto reservoir for monitoring the seismicity eventually induced by gas storage activities (Priolo et al., 2015). We specifically surveyed the deformed terraces of the Biadene windgap (Ferrarese et al., 1998), whose attribution varies in the literature from Early (Venzo et al., 1977) to Late Pleistocene and Holocene (Benedetti et al., 2000), with important consequences on the uplift rates of the MoA, and the shortening of the mountain front. In exploring these geomorphic features, we correlated them with the Pleistocene and Holocene fluvial terraces of the Northern Apennines, and their covering soils and colluvia (e.g., Gunderson et al., 2014; Picotti & Pazzaglia, 2008; Ponza et al., 2010; Wegmann & Pazzaglia, 2009).

A better definition of the geometry and kinematics of the mountain front of the eastern Southern Alps implies a wider understanding of the collisional history of the whole European Alps, still debated in terms of crustal/lithospheric geometries and timing. In this frame, our discussion on the shortening rates across the MT, averaged at different timescales, from 10^6 to 10^4 yr, has important bearings for the definition of the seismic hazard in this densely populated area.

2. Geological Context

The eastern Southern Alps are formed by two superposed fold and thrust belts (Figure 1): the first belongs to the frontal belt of the Dinarides, forming NW-trending structures, developed as pro-belt in the Eocene (Doglioni & Bosellini, 1987), but reactivated in the Late Oligocene to Early Miocene (Castellarin et al., 1992). The second, associated to ENE-trending structures, formed as the retro-belt of the Alps since the Middle Miocene, and it is considered still active in its frontal range (e.g., Castellarin et al., 1992), where the influence of the Dinaric structures is minor. The structural style of this frontal sector of the Alps offers the same problems of interpretation of many other mountain belts of the world (see Vann et al., 1986), due to the presence of possible blind thrusts and/or triangle zones. Several scholars published cross-sections of the study area, showing various angles of thrusting and degree of involvement of the basement, with consequent variations of the shortening amount (Figure 2; Castellarin et al., 1998; Doglioni, 1992; Roeder & Lindsey, 1992; Schönborn, 1999; Verwater et al., 2021). In particular, the structures of the frontal area around the Montello hill have been depicted by a seismic profile in Fantoni et al. (2002). Based on this and a previous work on the Montello area of Benedetti et al. (2000), Galadini et al. (2005) published a cross-section, where, differently from Castellarin et al. (1998), Doglioni (1992), and Schönborn (1999), they propose both the BV and the MT as two separate structures, formed by steep (>45°) ramps rooted in the basement. As visible in Figure 2 the structural styles and associated shortening estimates are very variable between authors. The new cross-sections presented in this paper, based on the main constraints from

10.1029/2022TC007522

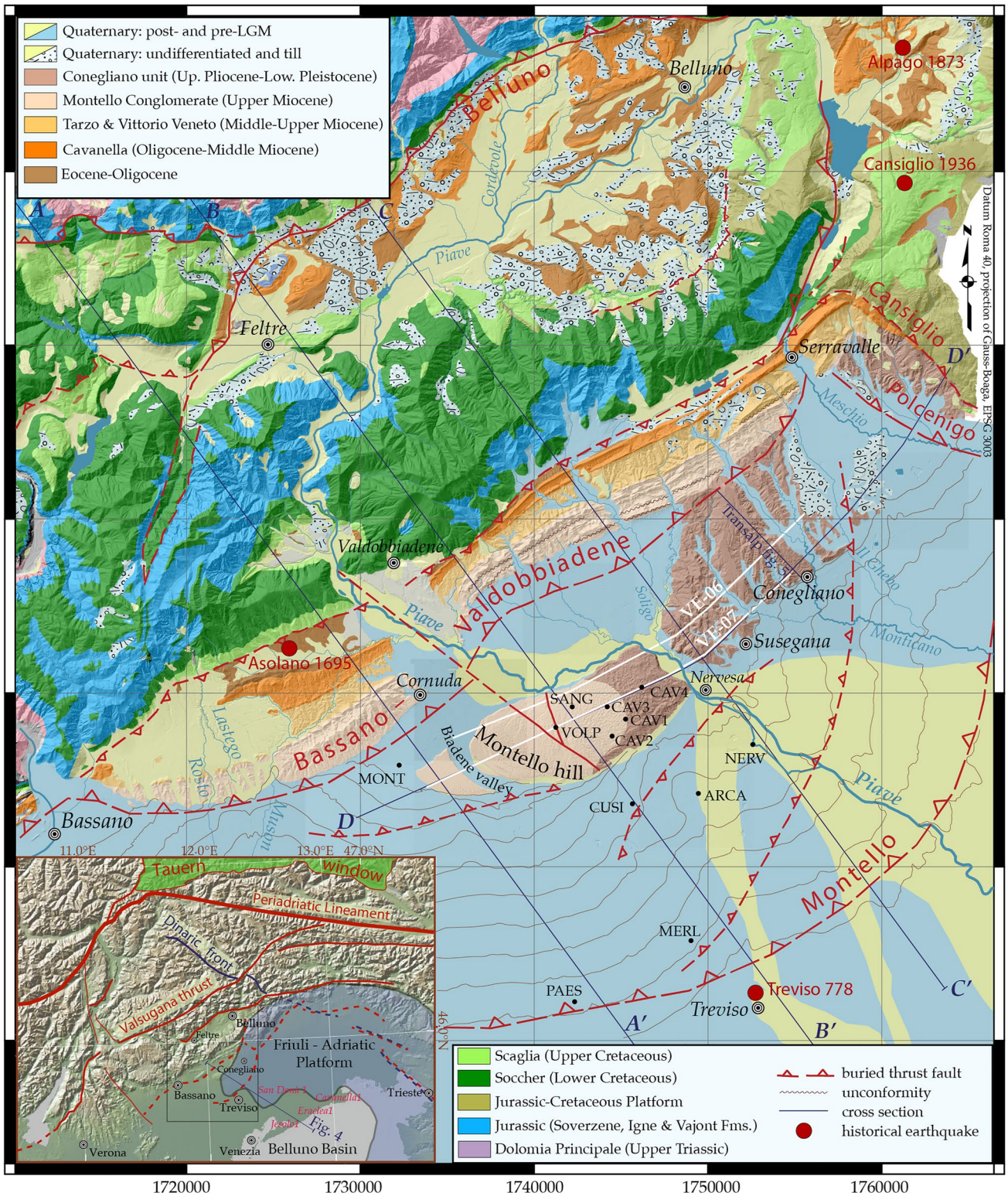

Figure 1. Geological sketch map of the studied sector of the eastern Southern Alps, with trace of the geological cross-sections and studied seismic sections as well as the main localities and wells quoted in the text. The buried structures are represented as vertical projection of the fault tip. The white tracks labeled VE-06 and VE-07 are the most significant industrial seismic profiles analyzed for this study. In the inset, note the margin of the Friuli-Adriatic Platform and the Belluno Basin, the Periadriatic Lineament with the tip of the Tauern Window and the front of the so-called Dinaric structures (blue lines, see Castellarin et al., 1992; Doglioni & Bosellini, 1987). Note the interference and reactivations with the middle Miocene to Present structures (red lines).

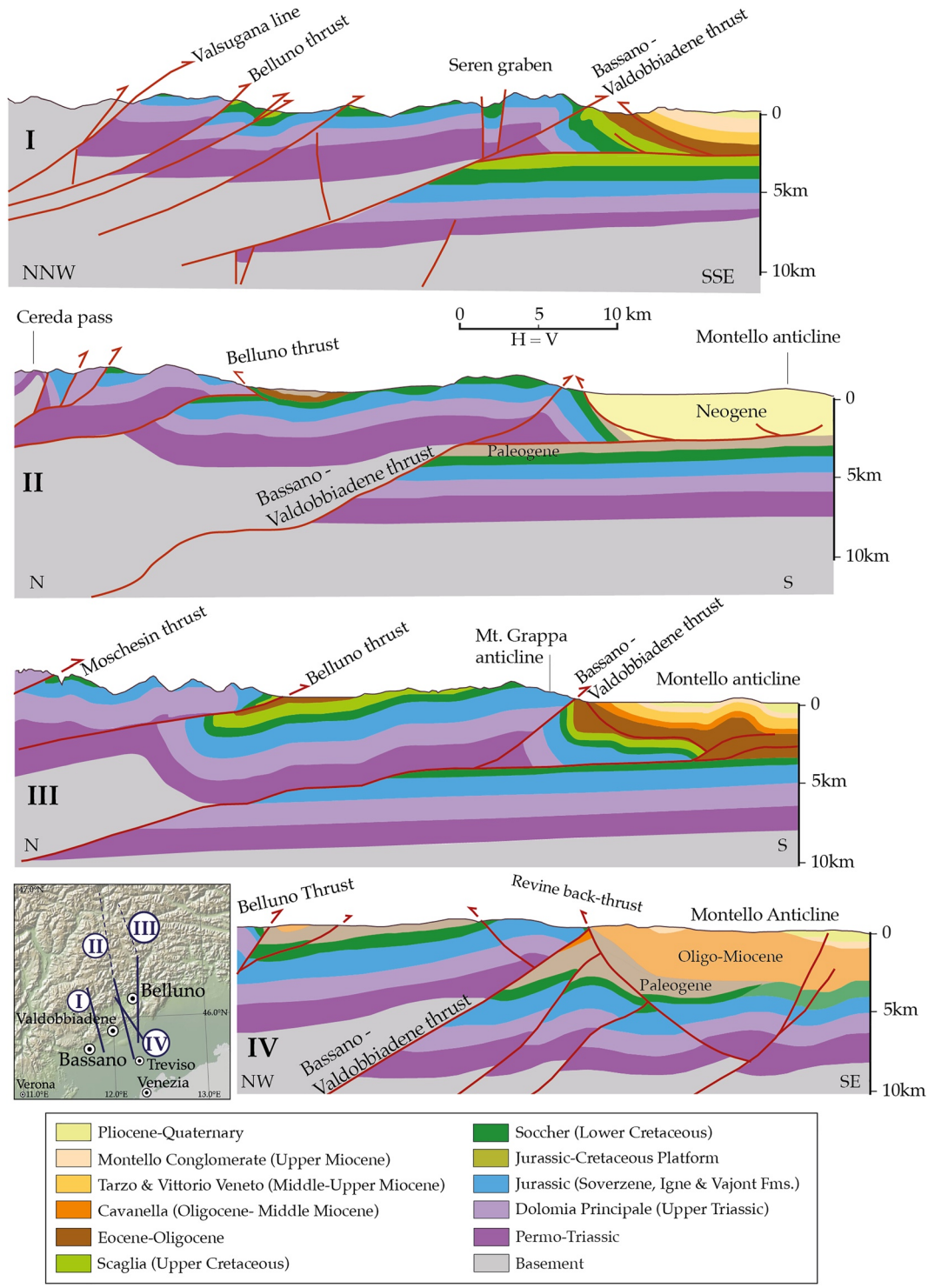

Figure 2. Structural style at the mountain front of the eastern Southern Alps around the Montello, according to various authors. (a) Doglioni (1992); (b) Castellarin et al. (1998); (c) Schönborn (1999); (d) Galadini et al. (2005).

surface and subsurface geology, will allow a deep discussion of the structural architecture of the mountain front of the eastern Southern Alps.

The contrast between the scarce seismicity north of the Periadriatic lineament (e.g., Reiter et al., 2018) and the intense activity at the front of the eastern Southern Alps is such that, in the recent past, several authors

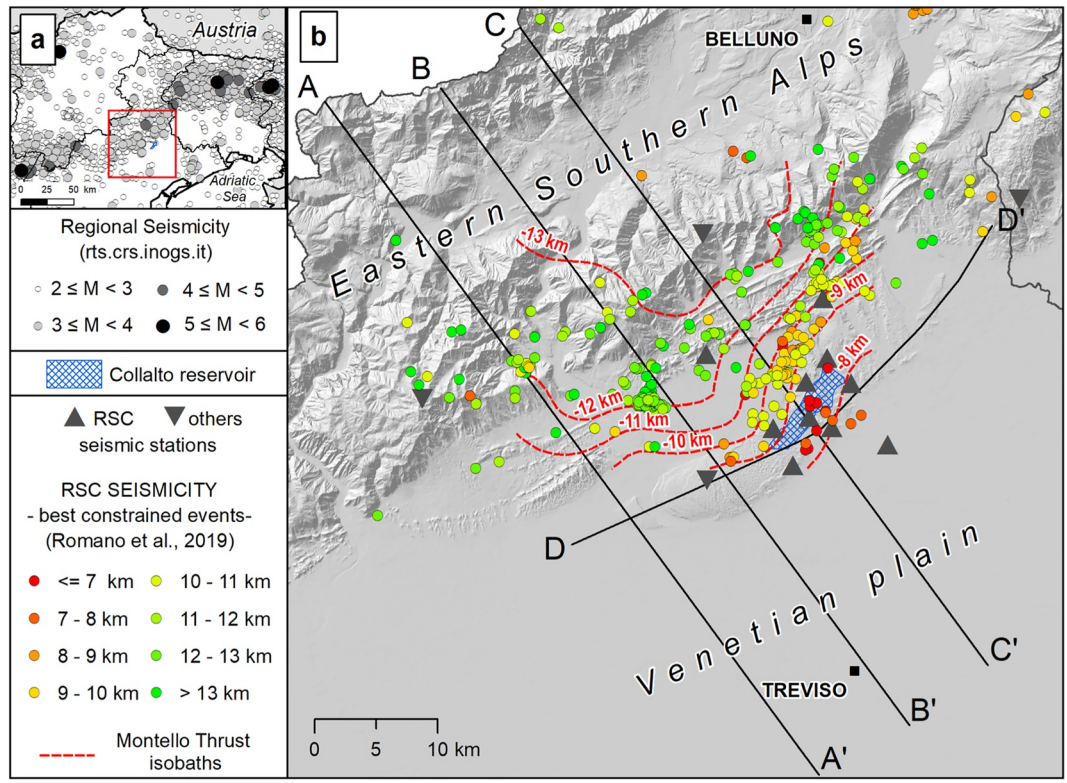

Figure 3. Map of the Montello thrust isobaths (depth below sea-level) constructed on the basis of RSC seismicity located from 1 January 2012 to 31 October 2017; note that only best constrained events are represented. Traces of the geological cross-sections AA', BB' CC', and DD' of Figure 6 are indicated. See text for details.

proposed the Southern Alps turned into a lower subducting plate in the last 14–15 Ma (e.g., Handy et al., 2015 and references therein). This idea was also supported by early tomographic data (Lippitsch et al., 2003), showing an apparent Adriatic slab dipping north. New experiments in the frame of the AlpArray project provided a different tomographic depiction of the subducting lithosphere in the eastern Alps, with the eastern Southern Alps still considered an upper plate (Handy et al., 2021). Nonetheless, the seismic activity at the front of the eastern Southern Alps still represents an anomaly in the larger frame of the Alpine orogeny. In this respect, the different shortening reconstructions proposed by various scholars (Figure 2) have direct implications for the amount of indentation of the Adria crust into the Alpine edifice. Larger shortening in the upper plate of Adria implies a more intricate indentation of the lithosphere against the European one. Eizenhöfer et al. (2021) in a collisional model based on integration of thermochronological with seismic and tomographic data, still propose a complex indentation of Adria, supportive of large shortening at the front of the eastern Southern Alps. Finally, Handy et al. (2021) showed negative *P* wave anomalies at the contact zone between Adria and Europe, which they interpret as delaminated lithosphere. This latter lithospheric configuration does not open the possibility of large shortening in the Adria-verging eastern Southern Alps.

The most striking feature of the Montello sector is the absence of historical strong earthquakes: no major event occurred between the 1695 Asolano earthquake (M 6.4, magnitude taken from ASMI, Rovida et al., 2017) and the 1873 Alpago (M 6.3) and Cansiglio 1936 (M 6.1) ones (Figure 1). Some moderate earthquakes occurred in the second half of XIX century, and, since 1977, few $3 < M < 4$ events (Figure 3a) have been recorded by the regional seismic network and by temporary monitoring (see Sugan & Peruzza, 2011 and references therein). The quality of the instrumental catalogs is non-uniform in time and space (Danesi et al., 2015; see Romano et al., 2019, and revised catalogs cited therein), till when, in 2011, a local dense network has been deployed to microseismically monitor the Collalto underground gas storage (Priolo et al., 2015).

In the years 1975–1985 the hydrocarbon industry explored the MoA, and, after drilling a well at the culmination of the anticline (well Volpago 1, Figure 1), they discovered and exploited the Conegliano gas field at Cavalletto

4. Interestingly, this gas field was found toward the eastern closure of the MoA. This fact has important bearing for the growth of the MoA. We will address this point in Sections 6 and 7 of this paper. After the depletion of the Conegliano gas field, the reservoir was turned into an Underground Gas Storage, named Collalto Storage, still operating, and microseismically monitored since 2012 (Priolo et al., 2015; Romano et al., 2019). Based on this monitoring, we present a reconstruction of the rock volume affected by microseismicity, providing constraints for the construction of the cross-sections (Section 5).

3. Material and Methods

We analyzed a grid of seismic reflection profiles, for a total of around 120 km acquired in the 70's last century, therefore at low resolution and aimed to illuminate the uppermost 2–3 km. This grid was kindly provided by Edison Stoccaggio S.p.A. Other parts of profiles were available as released industrial material. We based the construction of the cross-sections on field constraints, such as lithostratigraphic boundaries and faults, as well as bed attitude. Our field data were merged with the ones coming from the available official maps. The sketch map of Figure 1 represents a synthesis of these different sources. Our cross-sections, in their surficial part, are very similar to those already published constructed in the same area and presented in Figure 2. This point suggests that the field constraints are necessary but not sufficient for the deep interpolation of the subsurface geology. For this reason, we integrated in the profiles the geometries seen in seismics, calibrated by means of wells. These latter can be found on ViDEPI (2010), the website of available seismics and wells in Italy (ViDEPI, 2010), except for some of the wells still used for the storage (Collalto Storage), again provided by the storage company. The well stratigraphy in the Venetian plain was revised, taking into account the outcropping stratigraphy surveyed by Venzo et al. (1977). Nervesa 1, Arcade 1, Merlengo 1, and Paese 1 wells have been used to calibrate the seismic profiles.

The nature of the methane gas, a valuable tool to define its genesis and more generally the evolution of the MoA, was explored through carbon and hydrogen isotope data of the original gas found in the Collalto reservoir. Two samples were taken from the same level of the reservoir, not readapted as storage, and analyzed by the technicians of the CNR-IGG of Pisa (Italy). The gas was sampled on the 20 July 2006 with a trap consisting of alcohol at −80°, for excluding possible water, whereas on the 24 July 2006 with a trap cooled with liquid N_2, for excluding C_2, C_3, and C_4 phases. Standard errors were ±0.10 for the delta^{13}C and ±1.0 for the deuterium.

Three parallel profiles have been constructed across the mountain front, to obtain seriated geological cross-sections. Profile CC' runs few km to the west of the TransAlp profile, whose high-resolution seismics is reinterpreted after Fantoni et al. (2002). A fourth profile (DD') ties along strike the other ones; it is based on the seismic line VE07, and calibrated by means of Montebelluna 1, Volpago 1, Santi Angeli 1, Cavalletto 1, 2, 3, and 4 wells.

All the profiles are interpolated at depth, following a mixed chrono-lithostratigraphic subdivision of the sedimentary cover, whose thickness is inferred from wells and the outcrops of the two major Mesozoic domains, the Friuli-Adriatic Platform, and the Belluno Basin, recently reconstructed (Picotti & Cobianchi, 2017; Picotti et al., 2019). The surface and subsurface Neogene and Quaternary stratigraphy is based on the literature and the revision of well logs available on ViDEPI (2010). The geological cross-sections have been constructed adopting the outcropping structural style of the Southern Alps, such as basement thrust sheets and secondary décollements in the sedimentary cover (e.g., Doglioni, 1992; Picotti et al., 1995; Schönborn, 1999; Verwater et al., 2021). Clearly, uncertainties increase moving away from the surface or calibration points, that is, wells and seismic profiles.

In order to constrain the geometries of faults at depth, we use the seismicity catalog published by Romano et al. (2019) to construct the isobaths of the Montello seismogenic horizon, in this paper interpreted as the thrust plane (Figure 3). The catalog results from the seismic monitoring performed at a local scale in the Montello area by the Collalto seismic network (Rete Sismica di Collalto, RSC; Figure 3). This network has been designed and is still managed by OGS (Istituto Nazionale di Oceanografia e di Geofisica Sperimentale) on behalf of Edison Stoccaggio S.p.A., to monitor the seismicity potentially induced by gas storage activities in the Collalto reservoir. RSC is a high-resolution permanent network, consisting of a cluster of high-sensitivity stations deployed right above the reservoir, fully operating since 2012 (Priolo et al., 2015). Over the years, RSC has provided a detailed picture of the Montello area background seismicity, so far poorly known, and has demonstrated that the underground storage activities are not related to such microseismic events (Peruzza et al., 2022; Romano

Table 1
The Revision of the Late Neogene to Quaternary Stratigraphy of Some Wells Used for the Construction of the Cross-Sections (Original Available on ViDEPI, 2010), Compared to the Thickness of Units Outcropping Near Cornuda (After Venzo et al., 1977)

	Cornuda outcrop thickness	Nervesa 1 progressive	Arcade 1 progressive	Marlengo 1 progressive	Paese 1 progressive
Upper Pliocene to Pleistocene alluvial unit	~700 m	0–1,015 m	0–730 m	0–1,118 m	0–1,164 m
Lower to Upper Pliocene marine unit	200 m	1,015–1,080	730–780	1,118–1,185	1,164–1,321
Montello Conglomerate	1,340 m	1,080–1,265	780–965	1,185–1,440	1,321–1,460
Vittorio Veneto sandstone		>1,265	>965	>1,440	>1,460

et al., 2019). The RSC catalog used contains 1635 earthquakes ($-0.8 \leq M_L \leq 4.5$) localized with an optimized 1D velocity model in the period January 2012 to October 2017. The spatial pattern of these seismic events depicts a well-defined NNW dipping surface, with a slope changing from more than 40° at NE to less than 20° at SW, as clearly shown in the vertical cross-sections (Romano et al., 2019); this seismicity pattern is interpreted as the brittle expression of the MT surface.

For this work, we sampled, following the best constrained hypocenters, the thrust trace picking points on all the cross-sections provided by Romano et al. (2019), both along dip and along strike direction. Then, we imported the 3D picked points in ArcMap® and interpolated them through the Topo to Raster tool, choosing a raster resolution compatible with the vertical error associated to earthquake locations with a cell size of 1,000 m. Finally, we used the computed surface as input of the Contour tool to obtain isolines that join points of equal depth (isobaths in Figure 3).

4. Neogene to Quaternary Tectonic Stratigraphy of the Eastern Southern Alps: A Reappraisal

With the aim of highlighting the syn-tectonic character of the stratigraphic succession and constraining the main tectonic events, we propose in this section a synthesis of the stratigraphy of the Montello for its Neogene-Quaternary aspects, adopting and revising the work of previous authors dealing with outcropping units (e.g., Caputo et al., 2010; Massari et al., 1986, 1993; Mellere et al., 2000; Venzo et al., 1977) and wells (e.g., Mancin et al., 2007, 2009), integrated with our own revision of the stratigraphy of some wells, available on ViDEPI (2010) (Table 1). An exhaustive stratigraphic treatment of the study area is beyond the scopes of the present work, and we refer interested readers to the quoted literature.

Figure 4 shows the chronostratigraphic chart and the simplified geometries of the Tertiary to Quaternary units along a north-south transect across the mountain front and the Venetian plain, visible in the inset of Figure 1. Following a regional erosional event encompassing the latest Eocene and earliest Oligocene, whose full significance is still obscure, the sedimentation re-established in the Late Oligocene with shelf deposits. The age of the basal deposits is younger east- (Mellere et al., 2000) and south-ward (Figure 4), spanning the Aquitanian to the earliest Burdigalian in the southernmost area (Eraclea well, Mancin et al., 2007). These deposits, mostly carbonates, form four transgressive-regressive cycles, separated by minor unconformities and they are represented by various formations (Mellere et al., 2000), collectively named here as Cavanella Group, adopting the subsurface nomenclature. They are followed by hemipelagic marls, spanning the Langhian to the early Messinian, named Tarzo marls (Gallare marls in the subsurface). In the north, at the foothills, thick clastic deposits named the Vittorio Veneto sandstones (Figure 4) are found in the mid-upper Tortonian, followed by the Montello conglomerate (Massari et al., 1993), encompassing the latest Tortonian to early Messinian. Overall, they are interpreted as a prograding fan-deltaic system, fed by the Alpine rivers, with the Vittorio Veneto sandstones representing the marine part, whereas the Montello conglomerate, formed by interbedded conglomerates and mudstones with minor sandstones, represents the continental proximal fans. The overall geometry of these two units is wedge-like, thickening toward the north (Figures 4b and 4c). The Montello conglomerate is topped by a prominent unconformity, locally deeply erosional. The three megaunits, shelf carbonates of the Cavanella Group, the hemipelagic marls (Tarzo/Gallare) and the prograding deltas and fans (Vittorio Veneto sandstones and Montello conglomerate) can be interpreted as the classical foreland triad (e.g., Naylor & Sinclair, 2008; Sinclair, 1997) in

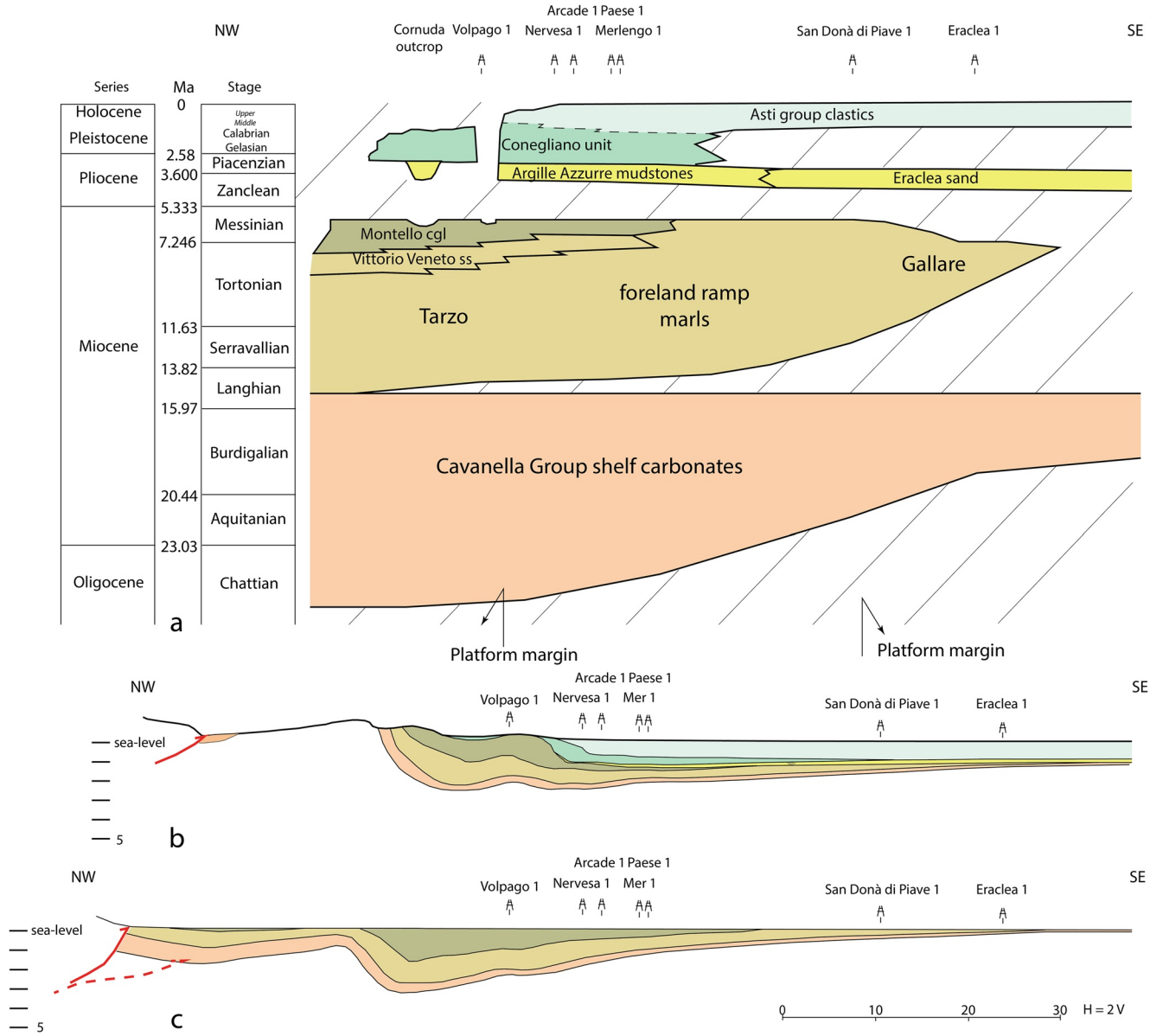

Figure 4. (a) Chronostratigraphic chart along an NW-SE belt on the study area. See Figure 1 for the location of the wells and the track of this profile. Ages taken from a stratigraphic revision of some wells (see Table 1) and literature quoted in the text. (b) 2X vertically exaggerated simplified cross-section, showing the wedge shape of the main clastic units (Vittorio Veneto sandstones (ss), Montello conglomerate (cgl), Conegliano unit). This wedge shape is not observed in the Asti Group; (c) reconstruction of the geology at the top Montello conglomerate (cgl) unit (end Messinian).

an overall shallow, overfilled basin. The northward thickening and the larger time gap in the south (Figure 4) do match with the establishment of a foreland flexure dipping to the north. As visible from the chronostratigraphic sketch of Figure 4, the Neogene units tend to thin and converge to the south toward the same inflection point, thus suggesting the bulge did not migrate through time (see retro-foreland basin of Bertotti et al., 1998 and Naylor & Sinclair, 2008).

The prominent erosional unconformity topping Montello conglomerate, associated to the base-level drop of the late Messinian, is documented by the Cornuda paleovalley (Venzo et al., 1977), incised for more than 400 m, and the reprocessed Transalp seismic profile of Fantoni et al. (2002). This latter (Figure 5) shows a rugged paleotopography covered by the Pliocene to Pleistocene Conegliano unit. Marine mudstones of the Argille Azzurre, bearing foraminiferal assemblages typical of the end of the Early Pliocene up to the beginning of the Late Pliocene, are found in local outcrops within the deeply incised paleovalley at Cornuda (Venzo et al., 1977). Deposits

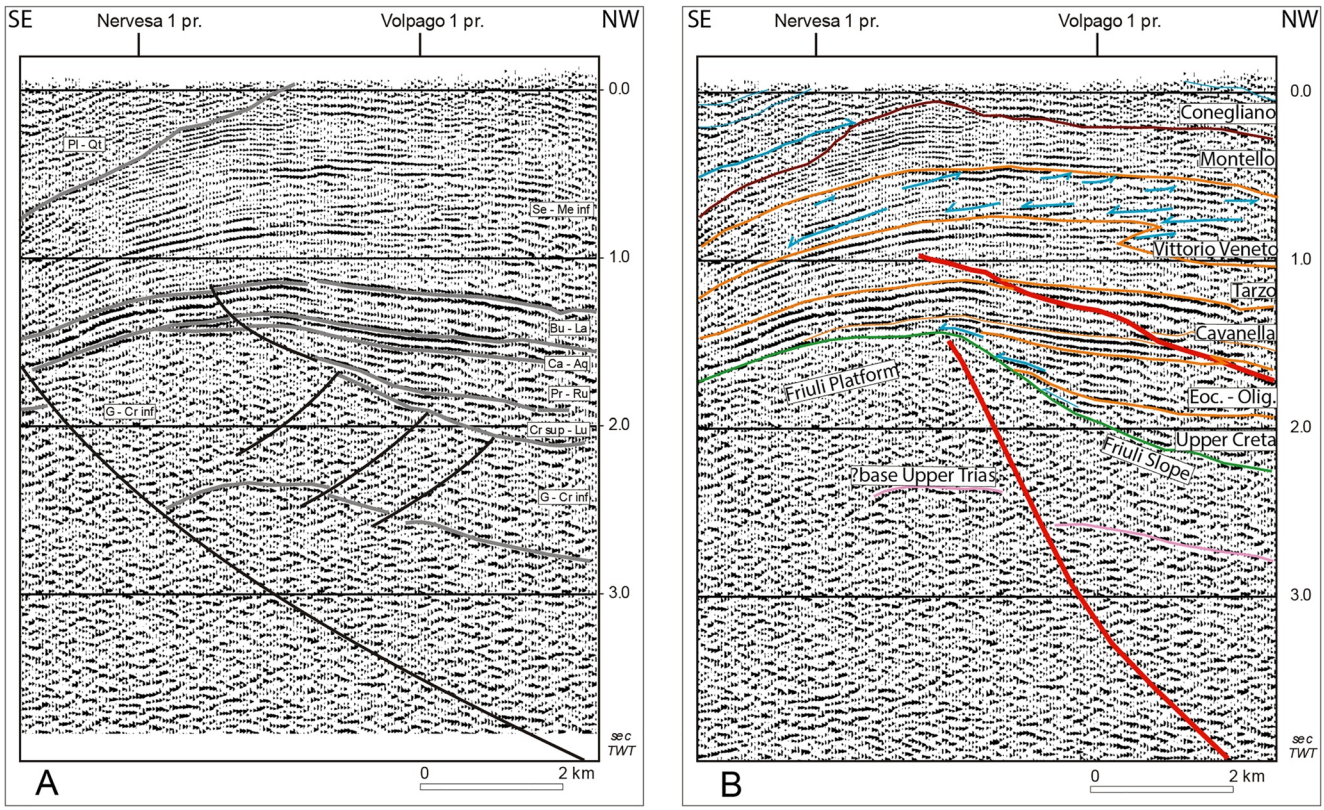

Figure 5. (a) Segment of the TRANSALP seismic profile reprocessed by Fantoni et al. (2002), crossing the Montello anticline (MoA), with their interpretation. (b) A slightly different interpretation proposed in this study; the brown line represents the rugged Messinian unconformity, separating the Montello conglomerate from the Conegliano unit; blue arrows on the top- and down-lap of the deltaic system of the Vittorio Veneto sandstone, prograding over the shelfal Tarzo marls. Underneath, one can observe the onlap of the basinal units onto the slope of the Friuli Platform.

of similar age are known at the foothills some 20 km to the west, near Bassano (Favero & Grandesso, 1982). This mudstone unit is observed also in the subsurface (Nervesa 1, Arcade 1, Marlengo 1, and Paese 1 wells, see Table 1), documenting the importance of the transgression and marine flooding on the eastern southalpine foreland in the end of the Early Pliocene. Since the recovery of the pre-Messinian sea-level, at the scale of the whole Mediterranean, occurred at the base of the Early Pliocene, this later transgression, recorded in the whole margin of the Southern Alps (Winterberg et al., 2020), points to a more regional control, still not fully understood. The Cornuda paleovalley was finally filled by a continental succession, spanning from lacustrine to alluvial (Venzo et al., 1977). This new continental unit of sandstones, mudstones and minor conglomerates covers, in the whole studied area, the deeply incised Montello conglomerate, as visible in the seismic profile of Figure 5. This latter unit was informally called Villafranchian conglomerate by Venzo et al. (1977) and Conegliano unit by Caputo et al. (2010). Around the Montello hill, the Montello conglomerate is unconformably covered by the Conegliano unit, with a clear onlap (Venzo et al., 1977). Although the two units are similar from a lithological point of view, they are clearly distinguishable in the topography, since the top of the Montello conglomerate is deeply weathered and strongly affected by karst (Ferrarese et al., 1998), contrary to the Conegliano unit. The time gap between the Montello conglomerate, deposited prior to the Messinian sea-level drop (occurring at around 6 Ma, e.g., Krijgsman et al., 1999), and the Conegliano unit, deposited after the marine transgression roughly calibrated at 3.8–2.9 Ma, is around 3 Ma. The climate in the Mediterranean between the end of the Messinian salinity crisis and the onset of the Pliocene was very wet and warm and characterized by very high precipitations (e.g., Willett et al., 2006). We refer to these climate conditions the deep weathering of the Montello conglomerate, expressed by paleokarstic dissolution in the gravel/conglomerate bodies. The Conegliano unit, as a matter of fact, is less weathered. The age of the top of the Conegliano unit in the outcrop is not well defined. Caputo et al. (2010) claimed the unit ended in the Early Pleistocene between 2.1 and 1.8 Ma, mostly based on the biostratigraphy of Fantoni et al. (2002). Immediately south of the Montello hill, in the Venetian plain, the sedimentation went on

till the Late Pleistocene and Holocene (Figure 1). Here, the Conegliano unit cannot be distinguished in the well records from the overlying clastics (collectively named Asti group, see Figure 4). Interestingly, the southernmost wells San Donà di Piave 1 and Eraclea 1 show a different stratigraphy (Mancin et al., 2007, 2009; Figures 1 and 4). Here, the Lower Pliocene transgressive deposits consist of sands, but the most important point is the missing deposition between around 3 and 1 Ma, when toward the north the Conegliano unit was forming. This suggests that the Conegliano unit still belongs to the northward thickening foreland units, similarly to the Late Miocene ones (Figure 4b). After 1 Ma, the geometry of the deposits changed from wedge-shaped and it appears more regular, with a slight thickening toward the south.

5. Geometry and Kinematics of the Mountain Front of the Eastern Southern Alps

The whole set of available information was used to construct geological cross-sections: the outcropping geology and available geological maps, the well stratigraphy and seismic profiles to constrain the shallow subsurface geology, and to locate the Belluno Basin-Friuli Platform boundary (Figure 1); the microseismicity pattern (Romano et al., 2019) and the MT isobaths, based on the best-constrained earthquake locations, to imagine the deep structural setting (Figure 3). The three seriated profiles along dip (AA', BB', and CC' in Figure 6) illustrate the MT as the frontal structure formed in sequence after the BV thrust. In our interpretation, this latter structure is a basement thrust sheet, creating an around 30 km long ramp anticline with asymmetric limbs, a northern gentle and a southern steep one. The hangingwall ramp flattens on a décollement level, hypothesized around the contact between the Cretaceous-Paleocene deep-water carbonates and the Tertiary clastics. The resulting style is typical of blind thrusts, with a triangle zone due to tectonic wedging, and passive roof layer-parallel backthrust (Price, 1986). A fourth profile (DD', Figure 6) crosses along strike the foothills of the Montello and adjacent area and illustrates the lateral termination of the MT and the transition of the eastern Cansiglio and Polcenigo-Maniago thrusts (see Galadini et al., 2005).

5.1. The Bassano-Valdobbiadene Thrust

The style of the Bassano-Valdobbiadene (BV) thrust is indeed typical of the frontal structures at the tip of many fold-and-thrust belts, where the deformation front interacts with the foreland basin, and it is controlled by the occurrence of décollement layers in the stratigraphy (e.g., Von Hagke & Malz, 2018). In the literature, tectonic wedging is widely acknowledged for the BV thrust (also named Grappa thrust) that has been interpreted as a thrust sheet formed by the sedimentary cover only, with a considerable shortening, >30 km according to Roeder and Lindsey (1992) or Schönborn (1999) (see Figure 2). Doglioni (1992), on the contrary, interpreted this main frontal thrust as a basement-cored structure, bearing a smaller shortening, around 12–14 km. In our sections, we choose the basement-core thrusting style according to Doglioni (1992) (Figure 6). Reason for that is the similitude with the other thrusts of the belt, especially the Valsugana and Belluno thrusts (e.g., Selli, 1998), associated with basement-cored anticlines and moderate shortening. In fact, our reconstructions suggest for the BV thrust around 14 km of shortening, in good accordance with Doglioni (1992), although our geometry of the thrust ramp is quite different. At Serravalle (Figure 1), the BV thrust turns into a lateral ramp, outcropping up to near Belluno. This left-lateral ramp merges the right-lateral ramp of the Cansiglio and Polcenigo-Maniago thrusts, creating a lateral ramp triangle, visible at the eastern side of Figure 1.

The age of the BV thrust can be deduced by the growing relationships with the stratigraphy. In fact, as visible in Figure 6, layer parallel geometries of the pre-Tortonian units document the ramp anticline of the BV thrust did not grow until Tortonian. Within the Vittorio Veneto sandstones and the Montello conglomerate of upper Tortonian to Messinian, several angular unconformities have been mapped, accompanying relevant thickness variations (Massari et al., 1986; Massari & Parea, 1988; Mellere et al., 2000). These unconformity surfaces are reported in Figure 1, and they pass laterally to conformities, depicting a trend of lateral variability of fold growth within 5–8 km. The oldest unconformity is visible to the east, and occurs at the base of the Vittorio Veneto sandstones, that is in the middle Tortonian, around 9.5 Ma (Mellere et al., 2000). Other evidence of growing stratigraphy is found toward the boundary and within the Montello conglomerate, documenting the BV thrust ramp grew between 9.5 and 6.5 Ma. Note that the evolution of the unconformities, and therefore the growth of the ramp structure, started earlier in the east, the area of thicker stratigraphy, and developed laterally toward the west. The youngest angular unconformity is locally found between the Montello conglomerate and the Conegliano unit (see

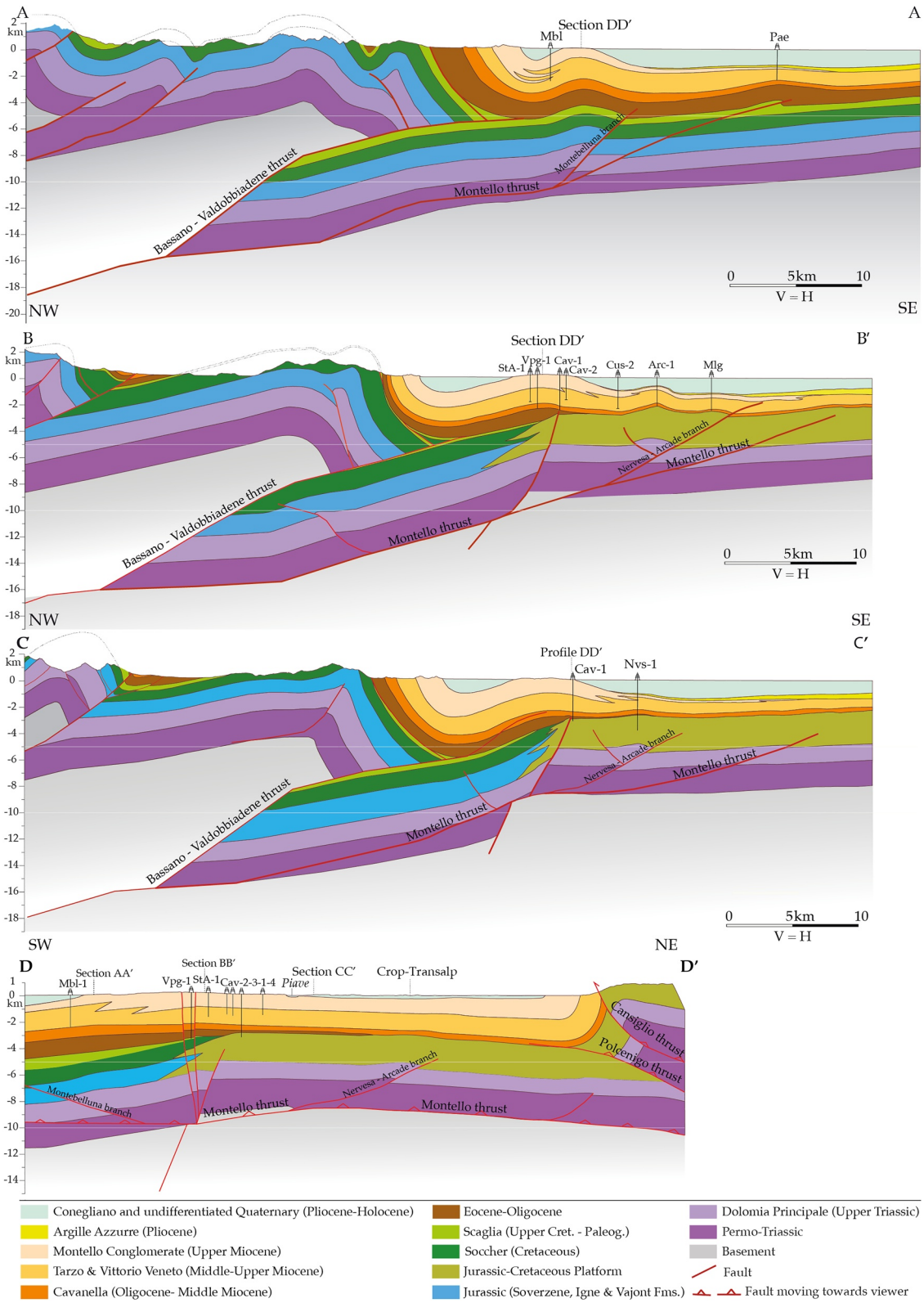

Figure 6. Structural style of the eastern Southern Alps illustrated through four geological cross-sections, oriented along dip (AA', BB', CC') and strike (DD') with respect to the belt. For location of cross-sections and calibrating wells, see Figure 1. See text for details.

Figure 1). The latter is still tilted south-ward, suggesting that the ramp anticline did not finish its limb rotation until recent times, and it is likely still forming.

5.2. The Montello Thrust

The MT is the most external structure of the eastern Southern Alps (Figures 1 and 6). It is associated to some anticlines, the largest of which is the MoA. The lower flat, as suggested by the distribution of the microearthquakes, is proposed at the base of, or within, the Permo-Mesozoic sedimentary cover. Toward the north, it merges with the BV thrust (Figure 6). The MT basal flat surface interacts with the normal fault separating the two Mesozoic domains, the Friuli Platform to the south, from the Belluno Basin north of it (e.g., Doglioni, 1992; Fantoni et al., 2002; Picotti & Cobianchi, 2017; Picotti et al., 2019). In our interpretation (section BB', Figure 6), the footwall tip of the Mesozoic normal fault was beheaded according to the geometry and kinematics of footwall shortcuts (e.g., Cooper et al., 1989; Hayward & Graham, 1989). The sedimentary succession on the hangingwall of the Mesozoic fault appears partially inverted, with the formation of the MoA (e.g., McClay & Buchanan, 1992; see Figure 5 and section BB' and CC' in Figure 6). The MT propagates southward, forming other two ramp anticlines of limited width, explored by some wells such as Paese 1 (Pae in sect. AA'), Arcade 1 and Merlengo 1 (respectively, Arc-1 and Mlg in sect. BB') and Nervesa 1 (Nvs-1 in sect. CC', Figure 6; see Figure 1 for location). The AA' profile crosses the Belluno Basin only and shows the MoA and associated ramp near its western closure. In this latter profile, therefore, the MoA consists of a pure ramp anticline, rather than an inverted rift structure. Toward the south, the anticline explored by the Paese 1 well documents the presence of a second branch of the MT. This southernmost branch of the MT is also visible in the profiles BB' and CC' and it extends southward till the outskirts of the town Treviso, as suggested by recorded very low to low-intensity earthquakes (Romano et al., 2019, see Figure 3; Jozi Najafabadi et al., 2021). The profile DD' cuts the MoA along strike and it shows the MT as an around 35 km wide structure. In this profile, the MT reaches maximum depth, around 10 km underneath the MoA, at the center between the profiles BB' and CC', rising both toward the west and the east, following the periclinal closures of the anticline. Profile DD' also shows the occurrence of two high-angle faults within the MoA, detected through the seismic profiles. In map view, these faults run NW toward the Piave valley (Figure 1), where the forelimb of the BV thrust appears clearly dragged in a left-lateral way. Given the abrupt thickness variations of the Upper Mesozoic to Tertiary on both sides of the Piave valley (compare profile AA' and BB'), it is very likely that these transcurrent structures derive from the reactivation of a Late Mesozoic to Tertiary west-dipping normal fault system. At depth along profile DD' (Figure 6), we do not have data to control their possible Late Mesozoic to Tertiary activity. Given the slight dip toward the east visible at the MoA in the seismic lines, these faults are interpreted to merge at depth with the Mesozoic normal fault. Finally, the profile DD' ends in the east against the lateral ramp of the Cansiglio and Polcenigo-Maniago thrusts, the kinematic equivalent, although shifted some 15 km to the south, of the BV thrust, with which it shares, in its lateral ramp, the same steeply tilted forelimb of the ramp anticline (see Figure 1 and profile DD').

The shortening associated to the MT can be assessed in the order of 2.5–3.5 km in its central portion, where we observe the maximum depths and three anticlines (profile BB' and DD', Figure 6). Toward its western closure (profile AA', Figure 6), the shortening decreases to around 1.5–2.5 km. In its central part, the thrust shows a minimum shortening of 3.5 km (average 0.4–0.5 mm/yr), 1.5 km associated to the Montello ramp/inverted fault, 1.25 km to the Arcade ramp and 0.75 km to its frontal part, not associated with any prominent ramp fold.

The age and evolution of the MT can be described by looking at the growth relationships of the stratigraphy and the evolution of beveling surfaces. The oldest proofs of the MT activity are around 8-6 Ma, provided by the growth relationships within the Montello conglomerate (see also Table 1). This topic will be deepened in the next section.

6. Onset and Evolution of the Montello Anticline

In literature, the MoA is considered a thrust cored anticline formed in the late Quaternary (Benedetti et al., 2000). Several lines of evidence document the MoA started developing during the sedimentation of the Montello conglomerate. Figure 7 represents its space-time evolution along the DD' profile, constructed with variable vertical exaggeration to enhance details. The profile runs along strike of the MoA and takes advantage from the

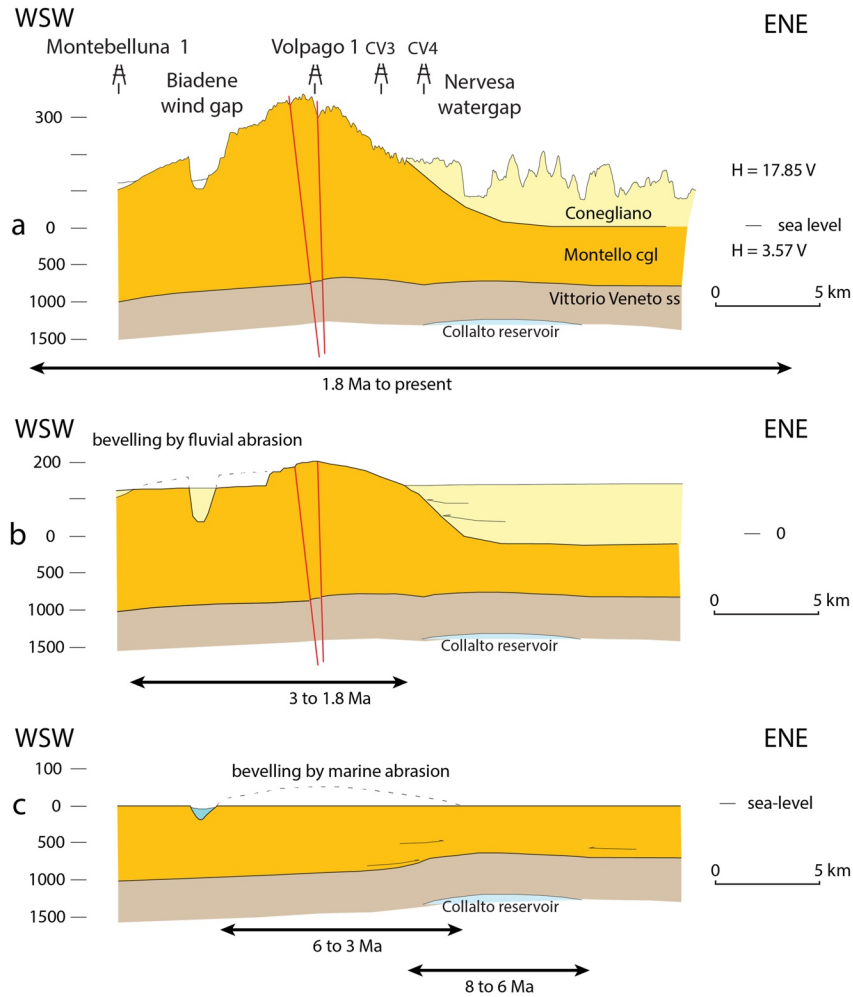

Figure 7. West-southwest to east-northeast cross-section of the Montello anticline, along the profile DD', based on wells and seismic profiles. Note the different vertical exaggeration above (x17.85) and below (x3.57) sea-level, in order to highlight both geomorphic features and subsurface geology. (a) Present-day, with the Collalto reservoir located east of the culmination. (b) Around 1.8 Ma, at the end of the Conegliano unit, onlapping the Montello conglomerate (cgl) toward the growing anticline, beveled to the west by fluvial abrasion. (c) At the maximum ingression of the sea, around 3 Ma, the Biadene paleovalley, formed at the Messinan drawdown, was infilled by sediments, and the growing anticline was abraded by the wave action. Note that the Collalto reservoir was formed earlier, between 8 and 6 Ma, prior to the western shift of the anticline growth. Black arrows indicate lateral termination of stratigraphy (onlap).

presence of several wells and a coincident seismic profile (see Figure 1) that constrain the thickness and geometry of the upper Miocene units.

Table 2
Isotopic Values of the Original Methane of the Collalto Reservoir

	Lab number	Sample	Date	‰ VS CO_2-PDB ^{13}C	‰ VS SMOW Deut
1	187893	COLLALTO	20.07.06	−67.16	−192.4
			24.07.06	−69.33	−184.5
2	187897	COLLALTO	20.07.06	−56.34	−213.1
			24.07.06	−59.76	−206.4

Worth noting is the occurrence of a gas field (Conegliano gas field), now depleted and transformed into an Underground Gas Storage (Collalto Storage). The reservoir consists of five isolated sandstone intervals, embedded in marly shales, of the Vittorio Veneto sandstones, located at around 1,210–1,320 m bsl at the culmination (Figure 7). The lateral closure of the levels, gently folded by the MoA is associated to pore tightening due to cementation, a process inhibited in the reservoir by the presence of the natural gas. The isotopic composition of this latter documents its biogenic origin (Table 2, compare with Schoell, 1980, 1988). The biogenic origin of the gas, and its occurrence in isolated levels separated by impermeable mudstones at the culmination of the MoA, collectively suggest the early diagenetic methanogenesis and its accumulation toward the anticline. This latter, therefore,

should have existed prior to the loss of porosity due to cementation and burial compaction, therefore already during the sedimentation of the overlying Montello conglomerate that provided the burial, that is, during the late Tortonian to early Messinian (8–6 Ma).

Interestingly, on the strike profile of Figure 7 one can appreciate that the gas field do not correspond to the present-day MoA axial culmination. Furthermore, the thickness of the Montello conglomerate is minimal at the Collalto reservoir top, and increases toward the Volpago 1, a dry well located around the present MoA axial culmination (Figure 7a). This difference in thickness is around 600 m in 5 km, documenting growing relationships toward the early culmination. Similar growth relationships, although less pronounced, occur along dip (see profile BB' in Figure 6) between the anticlines of Arcade and Marlengo (see Table 1). This documents that also the most external structures started growing during the Messinian, suggesting the MT was well developed at that time.

The Montello conglomerate ended its deposition due to the sudden drop(s) of the sea-level between 6 and 5.3 Ma, that strongly affected the Po-Venetian foreland basin (e.g., Amadori et al., 2018; Ghielmi et al., 2010). By observing that Biadene windgap is aligned with the paleovalley of Cornuda, well described by Venzo et al. (1977) and distant only 10 km to the north, we propose that it was carved at first during the same well-known Messinian drawdown, possibly by the same river carving at Cornuda (Figure 7a and Section 7.3). The paleovalley was then filled up by marine and continental deposits during the Pliocene transgression between 3.8 and 3 Ma (Venzo et al., 1977). This transgression brought the sea back at the southern foothills of the Alps as it is well documented by fiord-like occurrence of marine Pliocene deposits all along the western and eastern Sothern Alpine foothills (e.g., Favero & Grandesso, 1982; Venzo et al., 1977; Winterberg et al., 2020). During this time, the MoA was widening to the west and, in this context of shallow water abrasion, we observe around 100–200 m of erosion and beveling of the western sector of the anticline, suggested by the erosional unconformity between the Montello conglomerate and the overlying Conegliano unit as visible in the profile III of Venzo et al. (1977) (Figure 7a). Other authors dealing with the geomorphic evolution of the MoA (Ferrarese & Sauro, 2005) suggested the same amount of erosion.

The final Early Pliocene transgression started a new sedimentary cycle, forming the Conegliano unit (Caputo et al., 2010). After an initial marine to lacustrine environment in the Cornuda paleovalley, the proximal eastern Southalpine foreland basin was filled with conglomerates and finer clastics (see Figure 4, Fantoni et al., 2002; Venzo et al., 1977). The MoA kept growing toward the west, and the former culmination of the Collalto reservoir was covered with the Conegliano unit (Figure 7b). An Alpine river was beveling the westernmost tip of the anticline until the end of the deposition. The sedimentation, likely caused by an enhanced pluvial phase at the eastern Southalpine foothills (Villa et al., 2018), ended between 2.2 and 1.8 Ma (Caputo et al., 2010; Fantoni et al., 2002). After 1.8 Ma, the deposition of Conegliano unit in the study area ended, due to the MoA widening to the east and final uplifting.

6.1. Pliocene and Pleistocene Geomorphology of the Montello Anticline

The two erosional surfaces flooring and topping the Conegliano unit merge at the topographic culmination of the MoA, west of the closure of this unit (Figure 7). In this respect, this topographic surface corresponds to a complex erosional unconformity, developed during the last marine transgression, likely as wave abrasion platform, between 3.8 and 3.3–2.9 Ma, and then reworked in a continental environment afterward. This surface B1 (Figure 8), named T7 and T6 by Benedetti et al. (2000), is covered by 1–10 m red clay-rich lateritic soil, with interspersed rare deeply weathered siliceous and silicatic pebbles, the only insoluble remnant of the Montello conglomerate (Venzo et al., 1977). Thin veneers of loess occur, attributed by Venzo et al. (1977) to the Würm. The surface was uplifted during and after the deposition of the Conegliano unit, when the MoA was growing and the Conegliano unit onlapping against it (Figure 7b). During this first surface uplifting, synchronous with the Conegliano unit, the western part of the MoA was undergoing fluvial abrasion, with the formation of a second beveling surface (B2), which creates the top surface of the western half of the MoA (Figure 8). This surface, again covered by thick colluviated lateritic soil and thin veneer of loess, is considered middle to upper Pliocene (around 3–2 Ma) by Venzo et al. (1977), whereas it is named T5 and proposed 200 ky old by Benedetti et al. (2000). The transition between the two surfaces is only locally abrupt (Figure 8, profile 7), otherwise smooth (Figure 8, profile 6), as a result of slope degradation and soil colluviation. In the Venzo et al.'s (1977) interpretation, this local scarp

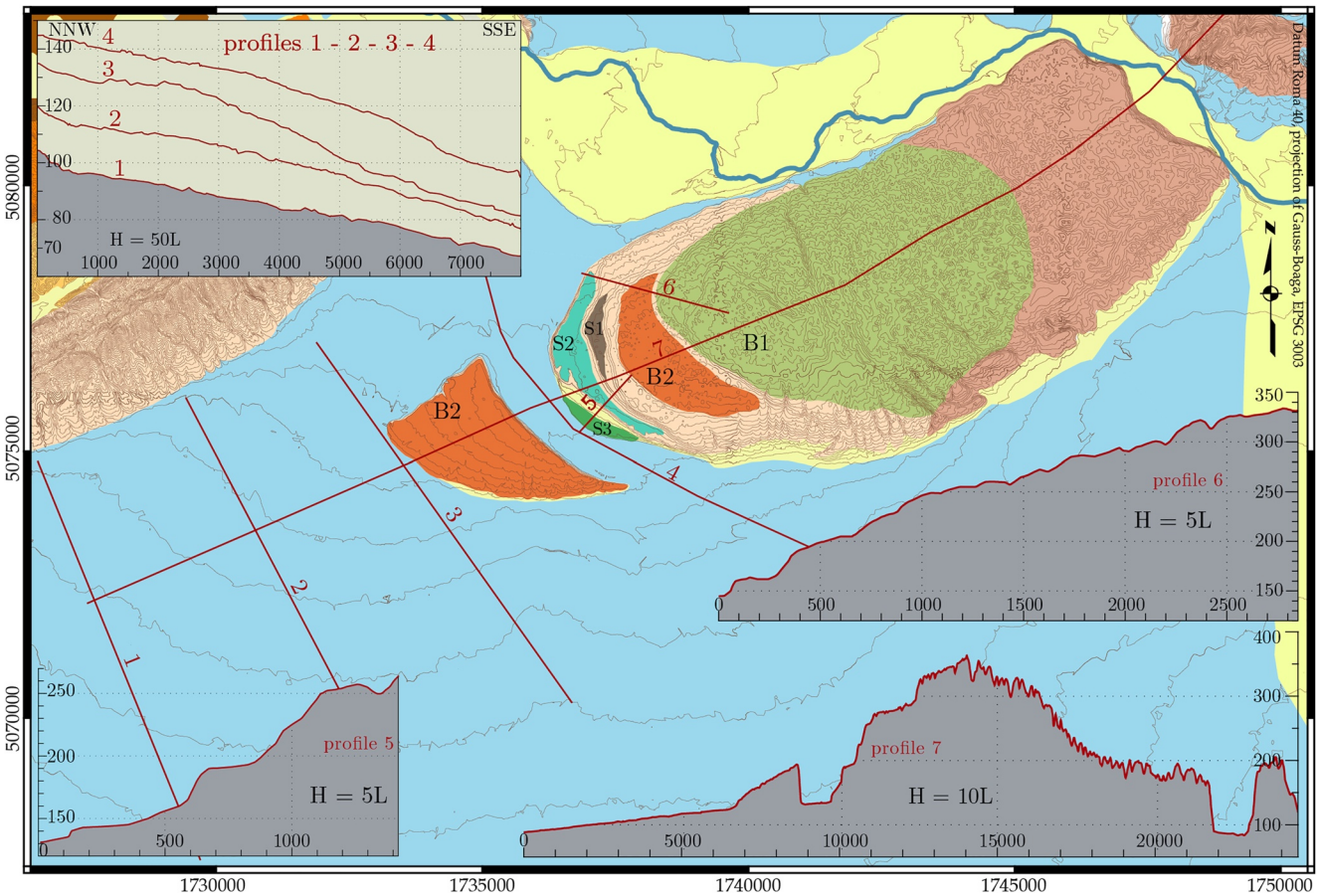

Figure 8. Geomorphic map of the Montello region, with topographic profiles, based on a high-resolution (5 m) DEM (https://idt2.regione.veneto.it/idt/downloader/download).

is inferred as tectonic in origin; a structural preconditioning seems the most likely explanation for this geomorphic feature that runs parallel to the strike-slip faults cutting through the MoA (Figures 1 and 8).

After the beveling of the two wide B1 and B2 abrasion surfaces, the river started incising epigenetically the former Messinian Biadene valley, and left three narrow strath terraces, separated by degraded risers, from the highest S1, S2, and S3 (Figures 7 and 8). These surfaces are again widely degraded and covered by thick colluvial wedges of red lateritic clay-rich soil, if we except the lower one. The top surface of the highest, named Günz by Venzo et al. (1977) and T3 by Benedetti et al. (2000), with less abundant dolines with respect to the B1 and B2 surfaces, is still covered by the thick lateritic clay-rich red soil (Ultisol), colluviated near the risers and dolines. The rare pebbles are silicatic only, and it is unclear if they are deriving from the degradation of the Miocene Montello conglomerate, or from Quaternary alluvial gravels. The same holds for the S2 terrace, Mindel for Venzo et al. (1977) and T2 for Benedetti et al. (2000) (see Figure 8). The lowest terrace S3 was named Riss (i.e., penultimate glaciation) by Venzo et al. (1977) and T1 by Benedetti et al. (2000). This latter, although covered by some 10 m thick wedge of colluviated red soil toward the riser, shows some rare weathered remnants of carbonate clasts interspersed with the silicatic ones. These lowest terraces are covered by a 1–3 m thick veneer of loess, consisting of yellowish silt to fine sand, slightly pedogenized. We never directly observed outcrops of alluvial fill, therefore we suspect that all of these terraces are strath only, as already discussed by Venzo et al. (1977).

Finally, the bottom of the Biadene windgap consists of a thick (at least 15–20 m) succession of gravels and sands of the Montebelluna fan, a pre-LGM feature in the Alpine foothills (Carton et al., 2009; Fontana et al., 2008). The unit is covered by a well-developed brown-orange soil, 60–80 cm thick, with limited carbonate Bk horizon. This soil correlates the ones on top of the Upper Pleistocene loess on the Apennine foothills and OSL dated at around 40 ky by Gunderson et al. (2014). It also correlates the soil topping the Qt4 of Picotti and Pazzaglia (2008),

Table 3
The Age Attribution of the Geomorphic Surfaces of Figure 8, Compared to Benedetti et al. (2000) and Venzo et al. (1977) Further Discussed in the Text

This work	Venzo et al. (1977)	Benedetti et al. (2000)	Max strath separation at culmination	Age Ma	Observables	Uplift rate mm/yr
			600 m	8–6	Thickness difference	0.3
			c.a 200 m	6–3	Erosion bottom Conegliano	0.08
B1	Pls	T7, T6	250 + 54 m k	3.3–2.9	Onlap Conegliano	0.1 ± 0.06
B2	Pls	T5	145 + 36 m k	2.1–1.8	Top Conegliano	0.094 ± 0.06
			159 m	1.8 to 0	Post Conegliano incision @Nervesa	0.09
S1	Günz	T3	96 ± 3	0.66 ± 0.08 MIS 16	Interpolated with 0.15 mm/yr	
S2	Mindel	T2	64 ± 1	0.45 ± 0.04 MIS 12	Interpolated with 0.15 mm/yr	
S3	Riss	T1	15 ± 0.5	0.13 MIS 6	Interpolated with 0.15 mm/yr	
Biadene windgap	Würm	T0	6.5 ± 0.5	27 ± 1 kyr MIS 2	Folded tread	0.24 ± 0.01

Note. The distances are measured between the tread of the Biadene windgap and the strath of the various surfaces, taken at the axial culmination of the Montello anticline. For the oldest surfaces B1 and B2, *k* means the thickness lost by karstic dissolution, see text for the methods. The age attribution of the oldest units is based on the stratigraphy, whereas the folding of the tread of Biadene windgap, OSL dated by Mozzi et al. (2015), is measured along the profile 4 of Figure 8 at the anticline culmination. Ages of terraces S1–S3 are interpolated with a mean value of 0.15 mm/yr, averaged between the Pliocene and the Würm values. See text for discussion.

which is dated at 40 ± 5 ky in Wegmann and Pazzaglia (2009). The Montebelluna fan was attributed to the early Würm (around 40 top 60 ky) by Venzo et al. (1977), thanks to the presence of paleontological findings, including mammoth bones. This dating was confirmed by a paleontological study of the bones by Reggiani and Sala (1992). A recent study (Mozzi et al., 2015) documents OSL ages of 37 ky at the bottom to 27 ky at the top of the Montebelluna fan, an age immediately preceding the LGM, slightly younger than previously discussed. The top of this fan in the Biadene paleovalley is folded around the MoA axis and its amplitude at culmination is 6.5 ± 0.5 m, based on the high-resolution DEM (see profile 4 in Figure 8).

7. Discussion

In this section, we will discuss the tectonic evolution of the eastern Southalpine mountain front, based on the data and observables synthesized on the cross-sections.

7.1. Age of Geomorphic Surfaces at Montello Anticline and Uplift/Propagation Rates

Based on the well-calibrated stratigraphy of Mozzi et al. (2015), the age of the top of the Montebelluna fan at Biadene windgap is constrained at 27 ± 1 ky (see Table 2). Given the anticline amplitude at the culmination in the Biadene windgap is 6.5 m, the resulting uplift rate is 0.24 ± 0.01 mm/yr. Benedetti et al. (2000) considered instead the Montebelluna fan as post-LGM, based on a Holocene (around 8 ky) radiocarbon dating of the mammoth bones, and the deformation of the top of the fan much higher, with a reconstructed uplift rate of around 1.4 mm/yr. The Benedetti et al. (2000) topography was much rougher and based on old 1:10,000 topo maps. The Holocene dating of the mammoth bones was rejected by all the scholars working in the region (e.g., Carton et al., 2009; Fontana et al., 2008; Marcolla et al., 2021; Mozzi et al., 2015; Reggiani & Sala, 1992). Accepting this date would rewrite the whole history of paleontology, youngest mammoth in Italy being dated 33.8 and 35.8 (Stuart et al., 2002) and Holocene mammoths never being found in central-southern Europe (Stuart, 2005).

To reconstruct the uplift rates of the MoA, we used different observables (Table 3). The 600 m thickness variations in the Montello conglomerate between 8 and 6 Ma document the growth of the early MoA by 0.3 mm/yr (Table 3). At this early time, the foreland subsidence rate was higher than the anticline uplift, with a final net subsidence of the area, including the MoA axial culmination. Both Ferrarese and Sauro (2005) and Venzo et al. (1977) agreed on around 200 m of erosion to create the B1 surface of Figure 8. This erosion occurred prior to its uplift, possibly due to marine abrasion and prior to the deposition of the Conegliano unit, between

6 Ma, onset time of the Messinian salinity crisis and drawdown of the base-level and 3.3–2.9 Ma, last important sea-level highstand in the Pliocene (Capozzi & Picotti, 2003). The anticline uplift rate, measured as elevation difference of the highest point of B1 and the surface of the Biadene windgap, is 0.08 mm/yr. Given the old age of the B1 and the underlying surfaces, to avoid underestimations, some correction should be considered. In fact, in karstic landscapes, such as the Montello hill, dissolution is relevant, as documented by the abundant dolines and the thick clay rich red soil (Ferrarese et al., 1998). Based on measured dissolution rates in similar climatic environment some 100 km to the east, Furlani et al. (2009) provided a surface lowering rate of 0.018 mm/yr in average. Although valid for the present-day interglacial time and for compact limestones, rather than calcareous conglomerates, this datum suggests the possible karstic lowering of the B1 surface of around 54 m. That would correct the uplift rate to 0.1 mm/yr (Table 3). The same correction was applied to the underlying B2 and S1 and S2 surfaces.

The top surface B1 started uplifting at 3.3–2.9 Ma, based on the age of the onlapping Conegliano unit, therefore we can confirm its Late Pliocene age, as first suggested by Venzo et al. (1977). The carving of the important surface B2 (Figure 8) in the western end of the MoA occurred during the deposition of the Conegliano unit, ending at around 2.1–1.8 Ma (see Section 4). Anticline beveling was effective in this setting, as it has been suggested in other foothills-fan environments (Bufe et al., 2016). The uplift rate of the surface B2 is 0.09 mm/yr (Table 3). By comparison, we can consider the Piave watergap in the eastern Montello end that is incising the Conegliano unit (see Figure 8). The elevation difference between the highest topographic point, minimum approximation for the top of the Conegliano unit (Collalto 243 m) and the present-day Piave river (84 m) provides a minimum incision rate of 0.09 mm/yr.

The strath surfaces, S1, S2, and S3 cannot be directly dated: adopting 0.15 mm/yr as minimum uplift rate, an average value between the end members, and the Furlani et al. (2009) average karstic surface lowering rate, their interpolated age would be 0.66 (MIS 16), 0.45 (MIS 12–11) and 0.13 (MIS 6–5) Ma, respectively (Table 3). The terrace S1, attributed to the Günz by Venzo et al. (1977), fall in the MIS 16 (ages of Bassinot et al., 1994). Although the original Günz terrace of Penck and Brückner (1909) is now considered MIS 24–22 (around 1–0.9 Ma, Knudsen et al., 2020), the MIS 16 is considered an important climatic deterioration (e.g., Bassinot et al., 1994), and traditionally in the Alps scholars refer to as Günz the glaciations occurred at MIS 16 (e.g., Van Husen, 2000). The recent paper of Knudsen et al. (2020) suggested the MIS 16 as the Mindel of Penck and Brückner (1909). The carving of the S1 terrace could be associated to that event, or, as an alternative, we could adopt for the interpolation of S1 the 0.1 mm/yr we obtained for the older B1 and B2 surfaces. In that case, S1 would fall into MIS 24–22, that would correspond to the Günz, according to Knudsen et al. (2020), therefore better fitting the Venzo et al. (1977) attribution. The interpolated age of the terrace S2, Mindel according to Venzo et al. (1977), falls at the transition MIS 12–11, adopting the 0.15 mm/yr average value. Adopting 0.1 mm/yr instead of 0.15 mm/yr as average uplift rate for this part of the MoA would bring the S2 to correlate to the MIS 16, recently proposed by Knudsen et al. (2020) as the Mindel of Penck and Brückner (1909), again better fitting the Venzo et al. (1977) attribution. The terrace S3 was considered Riss (penultimate glaciation) by Venzo et al. (1977), based on the Würm loess cover and the minor degree of weathering, with scattered presence of carbonate pebbles in the skeleton of the soil. The interpolated age of S3 (Table 3) well agrees with the Riss glaciation with both 1 or 1.5 mm/yr. The climatic conditions at the end of the MIS 6 are responsible also in the Northern Apenninic margin of wide fluvial terraces (e.g., Gunderson et al., 2014; Picotti & Pazzaglia, 2008).

Our reconstructed ages well agree with Venzo et al. (1977), but are way older than the ones proposed by Benedetti et al. (2000). The latter authors, unfortunately, based their time modeling of terraces on an unreliable radiocarbon age and on the assumption that fluvial terraces formed at every glacial-interglacial oscillation. The Benedetti et al. (2000) ages (Table 2), therefore, are way too young and the resulting MoA uplift rates, and associated shortening rates, higher by a factor 10.

Notwithstanding the uncertainties associated in the proposed age for the geomorphological features of the MoA, the uplift rates resulting from different stratigraphic methods, such as paleontology or radiometric/luminescence, are consistently steady around 0.1–0.2 mm/yr in the last 6 Ma. Only in the interval 8–6 Ma the early MoA relative uplift rates were 0.3 mm/yr. It is worth noting at that time, the width of the early MoA was very limited, in the order of 8.5 km.

The lateral propagation of the MoA, visible from Figure 7, is synthesized in Table 4.

Table 4
Lateral Growth of the Montello Anticline

Lateral growth rate Montello anticline			
Time intervals	Propagation distance km	Growth rate km/My	
8–6 Ma	8.5	4.25	Initial
6–3 Ma	9	3	Westward
3–1.8 Ma	4.2	3.5	Westward
1.8–0 Ma	30	16.7	Eastward

Note. See Figure 7 and text for discussion.

After the early (8–6 Ma) culmination of the MoA, propagating at a rate of 4.25 km/Ma, the fold propagated to the west by about 9 km in the time interval 6–3 Ma, showing a slightly decreased rate of 3 km/Ma (Table 4). The next time interval of 3–1.8 Ma shows a similar westward propagation at a rate of 3.5 km/Ma. The final step in the MoA evolution was a rapid eastward propagation occurred after 1.8 Ma, which brought about the end of the sedimentation of the Conegliano unit. The associated lateral growth rate is around 16 km/Ma. Although admittedly roughly reconstructed, Benedetti et al. (2000) reported lateral growth rate toward the west increasing from 10 to 20 km/Ma. However, those values are referred to an age assignment different from the present work (cf. Table 2). Another example of high-resolution quantification of the anticline lateral propagation is provided by Chen et al. (2007), who worked on a Kashi anticline at the southern front of the Tian Shan. In a context of frontal shortening rates of 1.5–1.9 mm/yr, the quoted authors found lateral growth rates of the anticlines variable from 40 to 80 km/Ma, decreasing to 15 km/Ma in the last 0.8 Ma.

Finally, the width of the MT as defined by the microseismicity (see Figure 3) matches the present lateral extent of the MoA (see Figure 1). As discussed previously, the early growth of the MoA was very likely due to the buckling and inversion of the Friuli slope succession (see Figure 5), therefore the MoA in its central part (Profile BB' and CC' in Figure 6) was possibly not cored by a thrust ramp. The post-1.8 Ma rapid propagation of the MoA to the east, reaching its final shape matching the width of the MT (see Figures 1 and 6), suggests that the MoA evolved as a fault-cored anticline during Pleistocene, and this change is possibly associated with the large post-1.8 Ma increase in propagation rate. The ramp responsible for this fold propagation is branching off the lower flat of the MT, as visible in the profile AA' and DD' (Figure 6). Whereas the early growth of the MoA followed the slope of the Friuli-Adriatic platform (profiles BB' and CC' in Figure 6), the post- 1.8 Ma thrust ramp and associated fold cut irrespectively of the previous paleogeographic domains, to the west entering the Belluno Basin (AA' in Figure 6) and to the east cutting into the Friuli-Adriatic Platform (see Figure 1 for the domain boundary). Since this ramp is branching from the deeper flat of the thrust, but is not the only one, with the Arcade and Paese anticlines further south, it appears difficult to associate a shortening to the MoA. However, this structure appears to account for most of the deformation, in the order of 2–3 km, with maximum centered around the profiles BB' and CC' (Figure 6).

7.2. Kinematics and Structural Style of the Active Mountain Front of the Eastern Southern Alps

In frontally accreting fold and thrust belts, it is common that the sedimentary cover of the upper crust gets detached, following rheologically weak layers, such as salt and/or shales, particularly at the base of the cover, where the overburden and the possibly associated fluid overpressure enhance their ductile behavior (e.g., Eocambrian at Salt Range, Jaumé & Lillie, 1988; Hormuz salt at Zagros, Molinaro et al., 2005; Triassic evaporites at Jura, Sommaruga, 1999). However, décollements in between the metamorphic basement and the sedimentary cover characterize other fold and thrust belts in the world, even in absence of evaporites (western USA, e.g., Fuentes et al., 2012). Shales and evaporites are usually found in the early stages of the marine transgression, therefore characterizing the base of the sedimentary succession that eventually will be involved in the compression. This is also the case of the eastern Southern Alps, where the latest Permian and earliest Triassic transitional facies are rich in shales and locally in evaporites. This interval is considered the main décollement in the case of the MT. A second regional transgression and associated local interval of décollement occur in the Carnian, at the base of the Dolomia Principale/Hauptdolomit. This secondary detachment surface is controlling the structural style in the inner part of the Southern Alps, but, in the frontal zone studied in this paper, it does not seem to have influenced the structural evolution of the thrusts, if present.

As pointed out by Lacombe and Bellahsen (2016), the thin- and thick-skinned styles of deformation are not mutually exclusive. In the eastern Southern Alps, the involvement of the basement in the thrust sheets is clear, since basement cored ramp anticlines occur in the main belt (e.g., Valsugana thrust, Selli, 1998). However, moving to the east toward the Friuli region, the spacing of the thrust sheets decreases dramatically (Figure 1, Largaiolli & Semenza, 1966), and the basement no longer shows up along the main thrust. This lateral variation is likely due

to the rheological changes at the expenses of the pre-Alpine basement, Variscan in origin, which grades to the east toward less- and non-metamorphosed terrains (Mariotto & Venturini, 2019). In the study zone, the thickness of the basement thrust sheet is hypothesized around 8 km, similarly to the proposal of previous authors. For the eastern Southern Alps, Schönborn (1999) proposed around 5 km, Doglioni (1992) around 7 km, whereas for the Giudicarie belt, both Picotti et al. (1995) and Verwater et al. (2021) proposed basement thrust sheets of 7–8 km in thickness. This thickness accounts for the spacing and width of the BV thrust sheet. The emplacement of this latter basement ramp in the late Miocene is kinematically associated with the Montello basal décollement at the base of the sedimentary cover. The involvement of basement and its thickness in the BV thrust is confirmed by Anselmi et al. (2011), who reconstructed the 3D velocity structure of the study area, based on local earthquakes tomography. Some of the smaller wavelength structures, visible in the cross-sections (Figure 6) between the Valsugana and the BV thrusts, could have been formed as thin-skinned propagation of the Valsugana basement ramp, whose evolution postdate the Langhian, the last marine deposit found in the deformation system (Castellarin et al., 1992; Selli, 1998).

As in other cases, for example, those reported by Lacombe and Bellahsen (2016), the deformation in the eastern Southern Alps evolves with the activation of basement thrusts, propagating up-section into large décollement at the base of the sedimentary cover, and minor flat (*sensu* Boyer & Elliott, 1982) at two intervals: within the Carnian, at the base of the Dolomia Principale/Hauptdolomit, and the Upper Cretaceous to Paleocene deep water units. The deeper basement thrust sheet passively uplifted and folded the previous thrusts and folds in the overlying sedimentary cover. This forward in-sequence propagation, with the active shortening presently occurring at the studied thrusts, Bassano-Valdobbiadene and Montello, is kinematically associated to the northward deepening of the deformation, arriving at around 30 km underneath the Periadriatic Lineament (Castellarin et al., 1998). Interestingly, recent geophysical data (Handy et al., 2021) indicate a relevant velocity gradient in the tomographic profile at the same depth underneath the Periadriatic Lineament, suggesting a possible detachment between the south verging middle-upper crust and the lower crust of Adria. Therefore, this makes it possible for the lower crust and the lithospheric mantle of Adria to be deformed and indented underneath the Alps for the equivalent of the around 35–40 km of shortening proposed for the middle-upper crust in the eastern Southern Alps (Castellarin et al., 1998; Schönborn, 1999). This configuration would be similar to that proposed for the central alpine profile and the western Southern Alps (e.g., Schmid et al., 1996). The Adria lower crust should be indented into the Alpine edifice in between the Periadriatic Lineament and the so-called sub-Tauern ramp (Gebrande et al., 2002, see Eizenhöfer et al., 2021; Reiter et al., 2018). The amount of shortening in the south-verging eastern Southern Alps should therefore match this distance, which increases from around 30 km in the west to more than 50 km in the eastern end of the Tauern Window, possibly due to the CCW rotation of the Adria indenter. This indentation is associated with dextral strike-slip faulting that becomes more relevant toward the east (e.g., Reiter et al., 2018; Serpelloni et al., 2016; Verwater et al., 2021). The range of total shortening proposed in the literature (35 km, Castellarin et al., 1998; >50 km Schönborn, 1999), therefore, very likely represent the two end members for the deformation in the eastern Southern Alps. Our reconstruction at the mountain front confirms or even decreases the shortening assessment of Castellarin et al. (1998), therefore pertaining to the minimum end member.

The structural style of the mountain front, with the BV ramp anticline and the associated blind thrust (Figure 6), has been interpreted by most authors as a passive roof wedging triangle zone (Boyer & Elliott, 1982; Von Hagke & Malz, 2018; see Figure 2). Our interpretation follows the same style, that appears the only one compatible with the missing south-verging fault plane at surface (Figure 1), and the abundant evidence of layer parallel shearing in the upper Cretaceous to Paleogene pelagic units in the frontal limb, suggesting the presence of an upper passive roof thrust (Figure 6). With respect to the triangle zone proposed by previous authors, in our sections the ramp is deeper, owing to the better calibration of the Miocene foreland deposits thickness and the microseismicity along the main detachment (Figure 3).

In map view, the BV thrust tapers to the east into a lateral ramp, forced by the reactivation of the Mesozoic platform margin of the Friuli Platform in its north trending part, including steeply dipping slope facies and normal faults (Figures 1 and 5, e.g., Doglioni, 1992; Picotti & Cobianchi, 2017). The frontal part of the BV thrust, however, is fully developed within the Belluno Basin. On the other hand, the MT cuts across the Mesozoic platform margin in its central part, and the pre-existing normal fault is not (or poorly) reactivated, rather passively cut by the thrust. The locking of normal faults in segments perpendicular with respect to the shortening direction is consistent with the mechanics of basin inversion (e.g., Sibson, 1995), which predicts fault reactivation and inversion only for structures with angles <30° to the shortening direction. An attempt to model the MoA as the inversion of

the deep-seated Mesozoic normal fault with a trishear geometry did not give plausible results. The inversion of a Mesozoic fault would create a narrower anticline, but with larger amplitude than the MoA, more similar to the easternmost lateral ramp of the BV ramp anticline (compare their geometries in the map of Figure 1). The MoA in its central part very likely formed due to buckling of the Paleocene to Miocene well-bedded interval of deep-water facies onlapping the slope of the Friuli Platform, that acted as buttress. However, it should be noted that the dip of the slope buttress, reconstructed in the cross-sections based on outcropping analogs (e.g., Picotti & Cobianchi, 2017; Picotti et al., 2019) and seismic profiles (Figure 5), is very similar to the one of the thrust reconstructed by Benedetti et al. (2000). The latter authors proposed a ramp of around 45°in the upper 5 km. The total shortening associated to MT varies from a 2.5–3.5 km in the central part of the thrust (section BB' in Figure 6) to around 1.5–2.5 km in the lateral part (section AA' in Figure 6). The uncertainties are due to the missing constraints in the subsurface and the shortening to be associated to the folds. Since the central part of the thrust started forming at 8 Ma, we can infer an average shortening rate for the MT of 0.3–0.4 mm/yr, a value 5 to 7 times less than the ones proposed by Benedetti et al. (2000). Recently, MT shortening rate was reconstructed, based on a dislocation modeling of the vertical geodetic deformation along the eastern Southalpine mountain front (Anderlini et al., 2020), calibrated with the new microseismicity data from Romano et al. (2019). Their estimated rate is 0.4 ± 0.1 mm/yr, in good agreement with the present work.

7.3. The Evolution of the Mountain Front Around Montello Hill: Interaction of Mountain Growth and River Incision

The frontal structures associated to the BV and MT evolved in a landscape dominated by rivers flowing southward from the growing alpine belt (Figure 9). At the middle Messinian, around 6 Ma, most of the catchments of the present rivers north of the Belluno thrust were already developed in their present-day location (Monegato et al., 2010; Winterberg et al., 2020). The occurrence of Permian rhyolitic tuff in the clasts of the Montello conglomerate west of Cornuda (Massari et al., 1993) documents the presence of a well-established catchment and similar erosional depths at the head of the Cismon creek already at the onset of Messinian (Figure 9a). The fan deltas sourced from the rising Alps were forming the Montello conglomerate at the depocenter of the Southalpine foreland basin. Both the BV and the early MoA were not emerging reliefs and their active growth was very likely controlling only the subsidence, hence the thickness, of the Montello conglomerate. The end Messinian drawdown of the Mediterranean (Figure 9b) brought about the carving of deep canyons in the previous fan deltas, as documented at Cornuda and its prolongation at Biadene. The Cismon creek was responsible for this incision. Further south, the Messinian incision of the river Brenta and Piave River was reconstructed from seismic profiles by Amadori et al. (2018). During the Early Pliocene transgression (Figure 9c), the MoA was beveled with the final formation of the B1 surface, and the rivers were carving in antecedent way the emerging relief of the BV ramp anticline. The Pliocene transgressive trend formed fiord-like coastlines, bringing marine sediments within the Messinian entrenched valleys, as documented in Cornuda (Venzo et al., 1977), Bassano (Favero & Grandesso, 1982) and Vittorio Veneto (Monegato et al., 2010). The Cismon creek was still responsible of the beveling of the western part of the MoA in the Early Pleistocene (Figure 9d), in a context of relevant deposition of pedealpine fans. We hypothesize the Cordevole river at that time carved a straight valley across the BV ramp anticline, forming the windgap of San Boldo pass (SB in Figure 9d) and continuing southward in the present Soligo valley to carve the watergap at Nervesa, presently occupied by the Piave river (compare Figures 9d and 9e). The windgap of San Boldo pass has been uplifted to 712 m asl, around 550 m higher than the thalweg. Taken as constant the uplift rate reported for the area from geodetic analysis, higher than 1 mm/yr (Anderlini et al., 2020), the diversion of the Cordevole and uplift has to be considered Middle Pleistocene. A former Cordevole in the present Soligo valley (see Figure 1) could also explain the occurrence of the large watergap at Nervesa, later captured by the Piave River. In the Middle and Late Pleistocene, the drainage reorganized to the present-day configuration, interplaying with the final growth and uplift of the MoA. The Piave was diverted by the continuous growth of the BV ramp anticline, flowing at the bottom of the syncline, merging with the Cordevole and entering the Cismon valley. The latter had a complex glacial/interglacial flow history toward the Piave and the Brenta catchments and was finally diverted into the Brenta River during the large flood of the 589 CE (Figure 9e; Rossato et al., 2018).

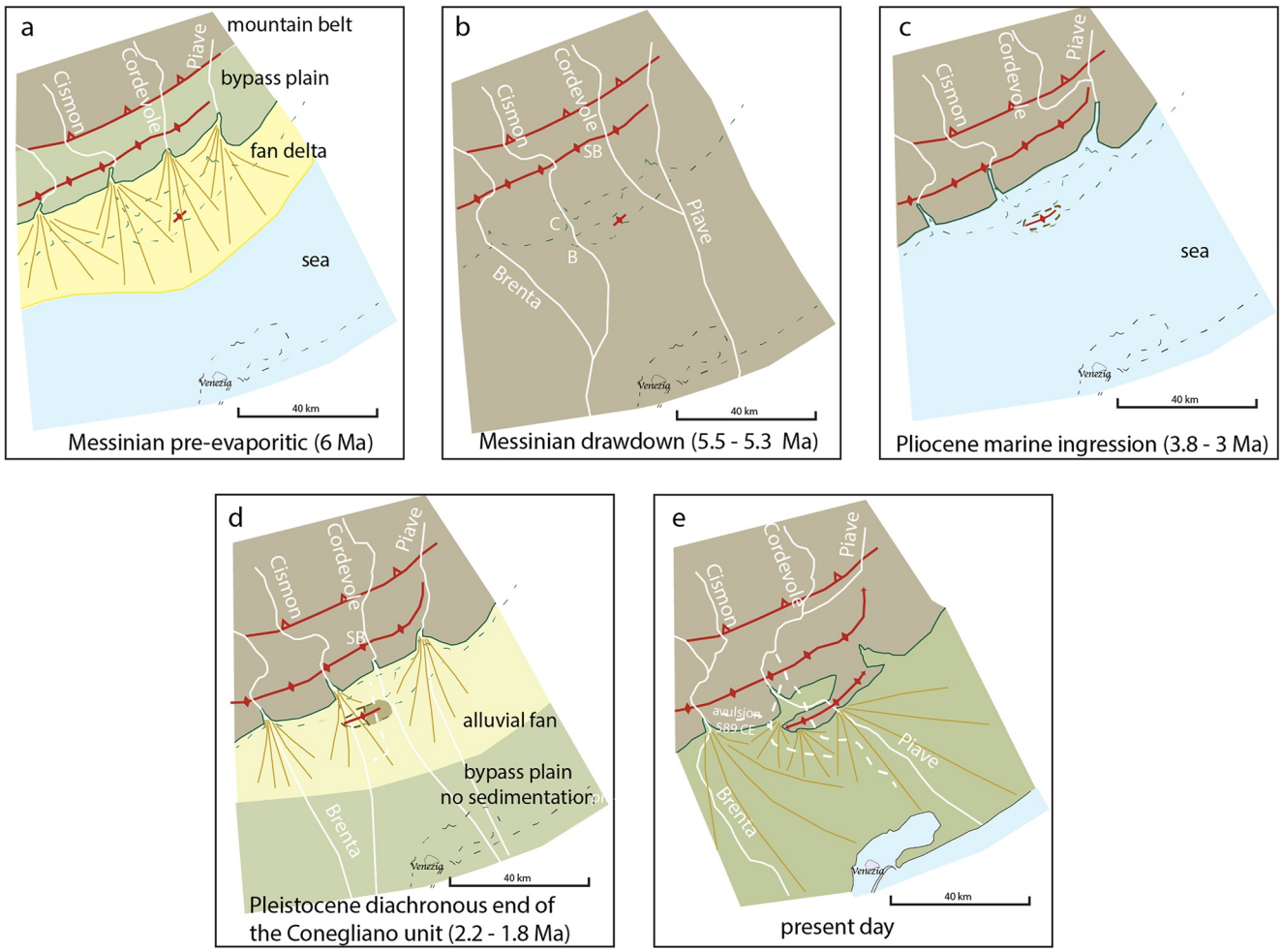

Figure 9. Competition between tectonic growth of the mountain front, river evolution and environments in the foreland, inspired from Monegato et al. (2010). (a) Pre-evaporitic Messinian: formation of the Montello conglomerate from coalescent fan deltas, sourced by the Piave, Cordevole and Cismon rivers, based on Massari et al. (1993). (b) The valley entrenchment at the Messinian drawdown and the formation of the Cornuda (C) and Biadene (B) and very likely the early San Boldo (SB) paleovalleys; the Brenta and Piave valley in the present Venetian plain are taken from Amadori et al. (2018). Note the incipient early Montello anticline (MoA). (c) At the maximum sea ingression in the Pliocene, the Cordevole was possibly diverted into the Piave, as its Pliocene valley was never found. (d) During Pleistocene, the larger MoA was beveled from the Cismon fan, the Cordevole was carving the San Boldo and other windgaps across the BV ramp anticline. (e) The last sketch shows the present-day setting, with the path of the pre-LGM Piave-Cordevole-Cismon system and the final diversion of the Cismon in historic times (Rossato et al., 2018). Megafans after Fontana et al. (2008, 2014).

7.4. Seismotectonic Implications

Before the recent availability of well-recorded microseismicity (Danesi et al., 2015; Priolo et al., 2015; Romano et al., 2019), the area surrounding the Montello hill has been for a long-time considered a seismic gap or, at least, an area of low seismic rate (e.g., Burrato et al., 2008), inside the larger seismotectonic district Pedemontana Sud of Sugan and Peruzza (2011) that encompasses the mountain front till the Cansiglio thrust to the east (see Figure 1). The most recent revision on historical earthquakes (ASMI, Rovida et al., 2017) show only one moderate, occurred on 778 CE, and referred to as Treviso; some minor ($M < 5$) events in the late XIX century are located around the Piave river, west of Valdobbiadene (Figure 1). The Treviso 778 CE earthquake was discussed by Pettenati and Sirovich (2007), but, with only one intensity point given, they could not provide reliable constraints about its source. Based on the shortening estimates of Benedetti et al. (2000), some scholars considered the MT as potentially capable of generating M_w 6.5+ earthquakes (Burrato et al., 2008; DISS Working Group, 2021; Galadini et al., 2005; Poli et al., 2008). The new proposed geometry for MT, with a total area estimated over 1,000 km^2 ± 20%, about 60% of which ascribed to its flat portion, and 40% to the ramp, can host even events much larger (Wells & Coppersmith, 1994) than the ones historically observed, in case of full

rupture. Nonetheless, the assessment of the maximum possible rupture on a fault surface is still a debated topic and great caution should be used for quantitative estimation of magnitudes from fault dimension (e.g., Trippetta et al., 2019). Recent reviews of the geodetic deformation at the front of the eastern Southern Alps (Anderlini et al., 2020) show that both the BV and the MT are active, with most deformation accounted by the former one. A numerical model, based on the available geodetic data (Barba et al., 2013), suggested that the locked BV thrust has a greater seismic potential than the MT, which should slip as unlocked thrust mostly by creeping. Creeping behavior was hypothesized by Romano et al. (2019) too, based on observations of microearthquake distribution. The seismic potential of creeping faults in shallow continental crust was reviewed by Harris (2017), who documented cases of moderate to strong creeping faults earthquakes.

Our reappraisal of the geological data around the MoA suggests that the shortening associated with the MT is much lower than previously suggested by Benedetti et al. (2000). We cannot evaluate the active rates of shortening for the BV thrust, but we reconstructed the MT shortening for the segment associated to the MoA as 0.2 mm/yr. Even considering similar rates for the blind structures further south, for which we do not have data, we could reach maximum 0.3–0.4 mm/yr of shortening for the MT. These estimates well agree with the recent models based on the geodetic velocity field (Anderlini et al., 2020). Furthermore, our reconstructions of the geometry of the MT show that the southernmost tip of the thrust should be located at depth in the outskirts of the town of Treviso (see Figure 1). In our cross-sections, we noticed the structures associated with the MT are blind and their tip is located at 3–4 km at depth, therefore confirming the setting of the models of Anderlini et al. (2020) and Barba et al. (2013).

In conclusion, considering that most of the shortening at the front of Southern Alps is accounted by the BV thrust, that potential rupture patches are smaller for MT than BV, due to their different locking depth, and that creep may aseismically explain some deformation budget, in agreement with Slejko et al. (2008) we propose the major seismogenic potential is assigned to the BV thrust.

8. Conclusions

We revised the geology of the mountain front of the eastern Southern Alps, based on the integration of new and old surface and subsurface data, including microearthquakes, with the scope of redefining the growth, evolution and erosional history of the main thrusts and their seismic potential.

The MT represents the southernmost structure at the tip of the eastern Southern Alps. It is deeper than previously thought, a feature suggested recently also by Jozi Najafabadi et al. (2021). It started developing in late Tortonian and it is still active, as documented by both microseismicity (Romano et al., 2019) and geodesy (Anderlini et al., 2020). The thrust plane is well defined by microseismicity (Romano et al., 2019) and it is associated to the MoA and to other ramp folds southwards, buried in the Venetian plain. The tip of the MT reaches the outskirts of the city of Treviso. The MoA evolved as inversion of the former Friuli-Adriatic Platform margin and further grew laterally, following the thrust widening across the previous paleogeographic domains. The average shortening rate associated to the MT is 0.3–0.4 mm/yr, a value much lower than proposed in the literature.

The BV thrust developed from the early Tortonian (10–9 Ma) to present day and shows a minimum shortening of 14–16 km (average 1.4–1.7 mm/yr). Total long-term averaged shortening rate of the two active structures is 1.7–2.1 mm/yr, a value very close to the horizontal shortening detected from the integrated geodetic velocity field (Anderlini et al., 2020).

The mountain front has been carved by rivers starting from the Late Miocene, creating a succession of river captures and abandonments and consequent windgaps. The peculiar history of the MoA depends on river carving in the late Messinian, further Pliocene valley filling, and Pleistocene epigenetic carving, with the development of two wide beveling surfaces and three strath terraces on the Biadene windgap at the western part of the MoA. Our interpolated age constraints for the geomorphic surfaces of the MoA well agree with the ones proposed by Venzo et al. (1977).

The seismic potential for the mountain front of the eastern Southern Alps is moderate to high. However, both the BV and MT are active, they share the same deep décollement, and the former seems locked at higher depth whereas the second is freely slipping (Anderlini et al., 2020; Barba et al., 2013; Romano et al., 2019). They should

be considered as a complex system, whose seismic behavior and stress interferences have never been modeled and are still obscure. Understanding this system is needed for a better evaluation of the seismic hazard of the region.

Data Availability Statement

The regional seismic catalog of the study area represented in Figure 3a is available in rts.crs.inogs.it; the local microseismic catalog used for Figure 3b is available as electronic supplement in Romano et al. (2019); well data through ViDEPI (2010) (Figures 6, 7, Table 1); topo map through https://idt2.regione.veneto.it/idt/downloader/download and geological map data through ISPRA and Regione Veneto, http://gisgeologia.regione.veneto.it, https://www.isprambiente.gov.it/Media/carg/63_BELLUNO/Foglio.html.

Acknowledgments
The authors thank the staff of Edison Stoccaggio S.p.A., in particular Timur Gukov, for their kind collaboration and the access to the seismic and well data, and gratefully remember the late Ing. Raffaele Stefanelli for his kindness, scientific competence and sharpness. This work is dedicated to him. The isotope data for the methane were kindly provided by Edison Stoccaggio S.p.A. Frank J. Pazzaglia is thanked for the fruitful discussions and for sharing with us some field (bad) experience. Roberto Fantoni is thanked for discussions and for providing the reprocessed seismic profile of the Transalp project. We acknowledge discussions with Mark Handy and Eline Le Breton about the structural style of the Southern Alps. The use of the software system ArcMap®, developed by ESRI is acknowledged. The Associate Editor Ernst Willlingshofer, Andrea Billi and anonymous are thanked for their comments that improved the quality of the paper.

References

Amadori, C., Garcia-Castellanos, D., Toscani, G., Sternai, P., Fantoni, R., Ghielmi, M., & Di Giulio, A. (2018). Restored topography of the Po Plain-Northern Adriatic region during the Messinian base-level drop—Implications for the physiography and compartmentalization of the paleo-Mediterranean basin. *Basin Research*, *30*(6), 1247–1263. https://doi.org/10.1111/bre.12302

Anderlini, L., Serpelloni, E., Tolomei, C., De Martini, P. M., Pezzo, G., Gualandi, A., & Spada, G. (2020). New insights into active tectonics and seismogenic potential of the Italian Southern Alps from vertical geodetic velocities. *Solid Earth*, *11*(5), 1681–1698. https://doi.org/10.5194/se-11-1681-2020

Anselmi, M., Govoni, A., De Gori, P., & Chiarabba, C. (2011). Seismicity and velocity structures along the South Alpine thrust front of the Venetian Alps (NE-Italy). *Tectonophysics*, *513*(1–4), 37–48. https://doi.org/10.1016/j.tecto.2011.09.023

Barba, S., Finocchio, D., Sikdar, E., & Burrato, P. (2013). Modeling the interseismic deformation of a thrust system: Seismogenic potential of the Southern Alps. *Terra Nova*, *25*(3), 221–227. https://doi.org/10.1111/ter.12026

Bassinot, F. C., Labeyrie, L. D., Vincent, E., Quidelleur, X., Shackleton, N. J., & Lancelot, Y. (1994). The astronomical theory of climate and the age of the Brunhes-Matuyama magnetic reversal. *Earth and Planetary Science Letters*, *126*(1–3), 91–108. https://doi.org/10.1016/0012-821x(94)90244-5

Benedetti, L. P., Tapponnier, G., King, C. P., Meyer, B., & Manighetti, I. (2000). Growth folding and active thrusting in the Montello region, Veneto, northern Italy. *Journal of Geophysical Research*, *105*(B1), 739–766. https://doi.org/10.1029/1999jb900222

Bertotti, G., Picotti, V., & Cloetingh, S. (1998). Lithospheric weakening during "retro-foreland" basin formation: Tectonic evolution of the central South Alpine foredeep. *Tectonics*, *17*(1), 131–142. https://doi.org/10.1029/97tc02066

Boyer, S. E., & Elliott, D. (1982). Thrust systems. *AAPG Bulletin*, *66*(9), 1196–1230.

Bufe, A., Paola, C., & Burbank, D. W. (2016). Fluvial bevelling of topography controlled by lateral channel mobility and uplift rate. *Nature Geoscience*, *9*(9), 706–710. https://doi.org/10.1038/ngeo2773

Burrato, P., Poli, M. E., Vannoli, P., Zanferrari, A., Basili, R., & Galadini, F. (2008). Sources of M_w 5+ earthquakes in northeastern Italy and western Slovenia: An updated view based on geological and seismological evidence. *Tectonophysics*, *453*(1–4), 157–176. https://doi.org/10.1016/j.tecto.2007.07.009

Capozzi, R., & Picotti, V. (2003). Pliocene sequence stratigraphy, climatic trends, and sapropel formation in the Northern Apennines (Italy). *Paleogeography, Paleoclimatology, Paleoecology*, *190*, 349–371. https://doi.org/10.1016/s0031-0182(02)00614-4

Caputo, R., Poli, M. E., & Zanferrari, A. (2010). Neogene-Quaternary tectonic stratigraphy of the eastern Southern Alps, NE Italy. *Journal of Structural Geology*, *32*(7), 1009–1027. https://doi.org/10.1016/j.jsg.2010.06.004

Carton, A., Bondesan, A., Fontana, A., Meneghel, M., Miola, A., Mozzi, P., et al. (2009). Geomorphological evolution and sediment transfer in the Piave River system (northeastern Italy) since the last glacial maximum. *Géomorphologie: Relief, Processus, Environnement*, *15*(3), 155–174. https://doi.org/10.4000/geomorphologie.7639

Castellarin, A., Cantelli, L., Fesce, A. M., Mercier, J. L., Picotti, V., Pini, G. A., & Selli, L. (1992). Alpine compressional tectonics in the Southern Alps. Relationships with the N-Apennines. *Annales Tectonicae*, *6*(1), 62–94.

Castellarin, A., Selli, L., Picotti, V., & Cantelli, L. (1998). La tettonica delle Dolomiti nel Quadro delle Alpi Meridionali orientali. *Memorie Società Geologica Italiana*, *53*, 133–143.

Cheloni, D., D'Agostino, N., & Selvaggi, G. (2014). Interseismic coupling, seismic potential, and earthquake recurrence on the southern front of the Eastern Alps (NE Italy). *Journal of Geophysical Research: Solid Earth*, *119*(5), 4448–4468. https://doi.org/10.1002/2014jb010954

Chen, J., Heermance, R., Burbank, D. W., Scharer, K. M., Miao, J., & Wang, C. (2007). Quantification of growth and lateral propagation of the Kashi anticline, southwest Chinese Tian Shan. *Journal of Geophysical Research: Solid Earth*, *112*(B3), B03S16. https://doi.org/10.1029/2006jb004345

Cooper, M. A., Williams, G. D., De Graciansky, P. C., Murphy, R. W., Needham, T., De Paor, D., et al. (1989). Inversion tectonics—A discussion. *Geological Society, London, Special Publications*, *44*(1), 335–347. https://doi.org/10.1144/gsl.sp.1989.044.01.18

D'Agostino, N., Cheloni, D., Mantenuto, S., Selvaggi, G., Michelini, A., & Zuliani, D. (2005). Strain accumulation in the Southern Alps (NE Italy) and deformation at the northeastern boundary of Adria observed by CGPS measurements. *Geophysical Research Letters*, *32*(19), L19306. https://doi.org/10.1029/2005GL024266

Danesi, S., Pondrelli, S., Salimbeni, S., Cavaliere, A., Serpelloni, E., Danecek, P., et al. (2015). Active deformation and seismicity in the Southern Alps (Italy): The Montello hill as a case study. *Tectonophysics*, *653*, 95–108. https://doi.org/10.1016/j.tecto.2015.03.028

DISS Working Group. (2021). *Database of Individual Seismogenic Sources (DISS), Version 3.3.0: A compilation of potential sources for earthquakes larger than M* 5.5 in Italy and surrounding areas. Istituto Nazionale di Geofisica e Vulcanologia (INGV). https://doi.org/10.13127/diss3.3.0

Doglioni, C. (1992). The Venetian Alps thrust belt. In *Thrust tectonics* (pp. 319–324). Springer Netherlands. https://doi.org/10.1007/978-94-011-3066-0_29

Doglioni, C., & Bosellini, A. (1987). Eoalpine and Mesoalpine tectonics in the Southern Alps. *Geologische Rundschau*, *76*(3), 735–754. https://doi.org/10.1007/bf01821061

Eizenhöfer, P. R., Glotzbach, C., Büttner, L., Kley, J., & Ehlers, T. A. (2021). Turning the orogenic switch: Slab-reversal in the Eastern Alps recorded by low-temperature thermochronology. *Geophysical Research Letters*, *48*(6), e2020GL092121. https://doi.org/10.1029/2020GL092121

Fantoni, R., Catellani, D., Merlini, S., Rogledi, S., & Venturini, S. (2002). La registrazione degli eventi deformativi cenozoici nell'avampaese veneto-friulano. *Memorie della Societa Geologica Italiana*, *57*, 301–313.

Favero, V., & Grandesso, P. (1982). Nuovi affioramenti di Pliocene marino nei dintorni di Bassano del Grappa (Vicenza). *Memorie della Societa Geologica Italiana*, *24*(1), 71–77.

Ferrarese, F., & Sauro, U. (2005). La geomorfologia del Montello. In B. Castiglioni (Ed.), *Montello Karstic Cultural Landscape. Paesaggi carsici: Architettura di una relazione unica tra uomo e ambiente: Montello. Museo di Storia Naturale e Archeologia di Montebelluna* (pp. 27–39).

Ferrarese, F., Sauro, U., & Tonello, C. (1998). The Montello Plateau: Karst evolution of an alpine neotectonic morphostructure. *Zeitschrift für Geomorphologie*, *109*, 41–62.

Fontana, A., Mozzi, P., & Bondesan, A. (2008). Alluvial megafans in the Venetian-Friulian Plain (north-eastern Italy): Evidence of sedimentary and erosive phases during Late Pleistocene and Holocene. *Quaternary International*, *189*(1), 71–90. https://doi.org/10.1016/j.quaint.2007.08.044

Fontana, A., Mozzi, P., & Marchetti, M. (2014). Alluvial fans and megafans along the southern side of the Alps. *Sedimentary Geology*, *301*, 150–171. https://doi.org/10.1016/j.sedgeo.2013.09.003

Fuentes, F., DeCelles, P. G., & Constenius, K. N. (2012). Regional structure and kinematic history of the Cordilleran fold-thrust belt in northwestern Montana, USA. *Geosphere*, *8*(5), 1104–1128. https://doi.org/10.1130/ges00773.1

Furlani, S., Cucchi, F., Forti, F., & Rossi, A. (2009). Comparison between coastal and inland Karst limestone lowering rates in the northeastern Adriatic Region (Italy and Croatia). *Geomorphology*, *104*(1–2), 73–81. https://doi.org/10.1016/j.geomorph.2008.05.015

Galadini, F., Poli, M. E., & Zanferrari, A. (2005). Seismogenic sources potentially responsible for earthquakes with $M \geq 6$ in the eastern Southern Alps (Thiene-Udine sector, NE Italy). *Geophysical Journal International*, *161*(3), 739–762. https://doi.org/10.1111/j.1365-246x.2005.02571.x

Gebrande, H., Luschen, E., Bopp, M., Bleibinhaus, F., Lammerer, B., Oncken, O., et al. (2002). First deep seismic images of the Eastern Alps reveal giant crustal wedges and transcrustal ramps. *Geophysical Research Letters*, *29*(10), 921–924. https://doi.org/10.1029/2002GL014911

Ghielmi, M., Minervini, M., Nini, C., Rogledi, S., Rossi, M., & Vignolo, A. (2010). Sedimentary and tectonic evolution in the eastern Po-Plain and Northern Adriatic Sea area from Messinian to Middle Pleistocene (Italy). *Rendiconti Lincei*, *21*(1), 131–166. https://doi.org/10.1007/s12210-010-0101-5

Gunderson, K. L., Pazzaglia, F. J., Picotti, V., Anastasio, D. A., Kodama, K. P., Rittenour, T., et al. (2014). Unraveling tectonic and climatic controls on synorogenic growth strata (Northern Apennines, Italy). *The Geological Society of America Bulletin*, *126*(3–4), 532–552. https://doi.org/10.1130/B30902.1

Handy, M. R., Schmid, S. M., Paffrath, M., Friederich, W., & AlpArray Working Group. (2021). Orogenic lithosphere and slabs in the greater Alpine area-interpretations based on teleseismic *P* wave tomography. *Solid Earth*, *12*(11), 2633–2669. https://doi.org/10.5194/se-12-2633-2021

Handy, M. R., Ustaszewski, K., & Kissling, E. (2015). Reconstructing the Alps-Carpathians-Dinarides as a key to understanding switches in subduction polarity, slab gaps, and surface motion. *International Journal of Earth Sciences*, *104*(1), 1–26. https://doi.org/10.1007/s00531-014-1060-3

Harris, R. A. (2017). Large earthquakes and creeping faults. *Reviews of Geophysics*, *55*(1), 169–198. https://doi.org/10.1002/2016rg000539

Hayward, A. B., & Graham, R. H. (1989). Some geometrical characteristics of inversion. *Geological Society, London, Special Publications*, *44*(1), 17–39. https://doi.org/10.1144/gsl.sp.1989.044.01.03

Jaumé, S. C., & Lillie, R. J. (1988). Mechanics of the Salt Range-Potwar Plateau, Pakistan: A fold-and-thrust belt underlain by evaporites. *Tectonics*, *7*(1), 57–71. https://doi.org/10.1029/tc007i001p00057

Jozi Najafabadi, A., Haberland, C., Ryberg, T., Verwater, V. F., Le Breton, E., Handy, M. R., et al. (2021). Relocation of earthquakes in the southern and eastern Alps (Austria, Italy) recorded by the dense, temporary SWATH-D network using a Markov chain Monte Carlo inversion. *Solid Earth*, *12*(5), 1087–1109. https://doi.org/10.5194/se-12-1087-2021

Knudsen, M. F., Nørgaard, J., Grischott, R., Kober, F., Egholm, D. L., Hansen, T. M., & Jansen, J. D. (2020). New cosmogenic nuclide burial-dating model indicates onset of major glaciations in the Alps during Middle Pleistocene Transition. *Earth and Planetary Science Letters*, *549*, 116491. https://doi.org/10.1016/j.epsl.2020.116491

Krijgsman, W., Hilgen, F. J., Raffi, I., Sierro, F. J., & Wilson, D. S. (1999). Chronology, causes, and progression of the Messinian salinity crisis. *Nature*, *400*(6745), 652–655. https://doi.org/10.1038/23231

Lacombe, O., & Bellahsen, N. (2016). Thick-skinned tectonics and basement-involved fold-thrust belts: Insights from selected Cenozoic orogens. *Geological Magazine*, *153*(5–6), 763–810. https://doi.org/10.1017/s0016756816000078

Largaiolli, T., & Semenza, E. (1966). Studi geologici sulla zona di giunzione cadorina (Cadore orientale). *Studi Trentini di Scienze Naturali, Sezione A*, *13*(1), 157–199.

Lippitsch, R., Kissling, E., & Ansorge, J. (2003). Upper mantle structure beneath the Alpine orogen from high-resolution teleseismic tomography. *Journal of Geophysical Research: Solid Earth*, *108*(B8), 2376. https://doi.org/10.1029/2002JB002016

Mancin, N., Cobianchi, M., Di Giulio, A., & Catellani, D. (2007). Stratigraphy of the Cenozoic subsurface succession of the Venetian-Friulian Basin (NE Italy): A review. *Rivista Italiana di Paleontologia e Stratigrafia*, *113*(3), 401.

Mancin, N., Di Giulio, A., & Cobianchi, M. (2009). Tectonic versus climate forcing in the Cenozoic sedimentary evolution of a foreland basin (Eastern Southalpine system, Italy). *Basin Research*, *21*(6), 799–823. https://doi.org/10.1111/j.1365-2117.2009.00402.x

Marcolla, A., Miola, A., Mozzi, P., Monegato, G., Asioli, A., Pini, R., & Stefani, C. (2021). Middle Pleistocene to Holocene paleoenvironmental evolution of the south-eastern Alpine foreland basin from multi-proxy analysis. *Quaternary Science Reviews*, *259*, 106908. https://doi.org/10.1016/j.quascirev.2021.106908

Mariotto, P. F., & Venturini, C. (2019). Birth and evolution of the Paleocarnic Chain in the Southern Alps: A review. *International Journal of Earth Sciences*, *108*(8), 2469–2492. https://doi.org/10.1007/s00531-019-01774-y

Massari, F., Grandesso, P., Stefani, C., & Zanferrari, A. (1986). The Oligo-Miocene Molasse of the Veneto-Friuli region, Southern Alps. *Giornale di Geologia*, *48*(1e2), 235–255.

Massari, F., Mellere, D., & Doglioni, C. (1993). *Cyclicity in non-marine Foreland-basin Sedimentary fill: The Messinian conglomerate-bearing succession of the Venetian Alps (Italy)* (Vol. 17, pp. 501–520). Special Publications of the International Association of Sedimentologists.

Massari, F., & Parea, G. C. (1988). Progradational gravel beach sequences in a moderate-to high-energy, microtidal marine environment. *Sedimentology*, *35*(6), 881–913. https://doi.org/10.1111/j.1365-3091.1988.tb01737.x

McClay, K. R., & Buchanan, P. G. (1992). Thrust faults in inverted extensional basins. In *Thrust tectonics* (pp. 93–104). Springer. https://doi.org/10.1007/978-94-011-3066-0_8

Mellere, D., Stefani, C., & Angevine, C. (2000). Polyphase tectonics through subsidence analysis: The Oligo-Miocene Venetian and Friuli Basin, north-east Italy. *Basin Research*, *12*(2), 159–182. https://doi.org/10.1046/j.1365-2117.2000.00120.x

Molinaro, M., Leturmy, P., Guezou, J. C., Frizon de Lamotte, D., & Eshraghi, S. A. (2005). The structure and kinematics of the southeastern Zagros fold-thrust belt, Iran: From thin-skinned to thick-skinned tectonics. *Tectonics*, *24*(3), TC3007. https://doi.org/10.1029/2004TC001633

Monegato, G., Stefani, C., & Zattin, M. (2010). From present rivers to old terrigenous sediments: The evolution of the drainage system in the eastern Southern Alps. *Terra Nova*, *22*(3), 218–226. https://doi.org/10.1111/j.1365-3121.2010.00937.x

Mozzi, P., Rossato, S., Pascucci, V., Andreucci, S., Monegato, G., Fontana, A., & Sechi, D. (2015). Aggradation of the Montebelluna megafan (NE Italy) at the MIS 3-2 transition, problems, and perspectives. In G. Monegato, F. Gianotti, & M. G. Forno (Eds.), *Abstracts Volume AIQUA Congress 2015: The Plio-Pleistocene continental record in Italy: Highlights on stratigraphy and neotectonics* (Vol. 26, pp. 33–34). Miscellanea INGV. https://doi.org/10.13127/misc/26

Naylor, M., & Sinclair, H. D. (2008). Pro-versus retro-foreland basins. *Basin Research*, *20*(3), 285–303. https://doi.org/10.1111/j.1365-2117.2008.00366.x

Penck, A., & Brückner, E., (1909). *Die Alpen im Eiszeitalter* (Vol. 3, p. 1199). Tauchnitz, Leipzig.

Peruzza, L., Poli, M. E., Rebez, A., Renner, G., Rogledi, S., Slejko, D., et al. (2002). The 1976–1977 seismic sequence in Friuli: New seismotectonic aspects. *Memorie della Societa Geologica Italiana*, *57*, 391–400.

Peruzza, L., Romano, M. A., Guidarelli, M., Moratto, L., Garbin, M., & Priolo, E. (2022). An unusually productive microearthquake sequence brings new insights to the buried active thrust system of Montello (Southeastern Alps, northern Italy). *Frontiers of Earth Science*, *10*. https://doi.org/10.3389/feart.2022.1044296

Pettenati, F., & Sirovich, L. (2007). Was the Montello structure responsible for the 778 AD and 1695 earthquakes in the Veneto Region? New answers from the KF seismic hazard Scenario. GNGTS–Atti del 23° Convegno Nazionale/6 July 2007.

Picotti, V., & Cobianchi, M. (2017). Jurassic stratigraphy of the Belluno Basin and Friuli platform: A perspective on far-field compression in the Adria passive margin. *Swiss Journal of Geosciences*, *110*(3), 833–850. https://doi.org/10.1007/s00015-017-0280-5

Picotti, V., Cobianchi, M., Luciani, V., Blattmann, F., Schenker, T., Mariani, E., et al. (2019). Change from rimmed to ramp platform forced by regional and global events in the Cretaceous of the Friuli-Adriatic Platform (Southern Alps, Italy). *Cretaceous Research*, *104*, 104177. https://doi.org/10.1016/j.cretres.2019.07.007

Picotti, V., & Pazzaglia, F. J. (2008). A new active tectonic model for the construction of the Northern Apennines mountain front near Bologna (Italy). *Journal of Geophysical Research*, *113*(B8), B08412. https://doi.org/10.1029/2007JB005307

Picotti, V., Prosser, G., & Castellarin, A. (1995). Structures and kinematics of the Giudicarie-Val Trompia fold and thrust belt (central Southern Alps, northern Italy). *Memorie di Scienze Geologiche*, *47*, 95–109.

Poli, M. E., Burrato, P., Galadini, F., & Zanferrari, A. (2008). Seismogenic sources responsible for destructive earthquakes in north-eastern Italy. *Bollettino di Geofisica Teorica ed Applicata*, *49*, 301–313.

Ponza, A., Pazzaglia, F. J., & Picotti, V. (2010). Thrust-fold activity at the mountain front of the Northern Apennines (Italy) from quantitative landscape analysis. *Geomorphology*, *123*(3–4), 211–231. https://doi.org/10.1016/j.geomorph.2010.06.008

Price, R. A. (1986). The southeastern Canadian Cordilleran thrust faulting, tectonic wedge, and delamination of the lithosphere. *Journal of Structural Geology*, *8*(3–4), 239–254. https://doi.org/10.1016/0191-8141(86)90046-5

Priolo, E., Romanelli, M., Plasencia Linares, M. P., Garbin, M., Peruzza, L., Romano, M. A., et al. (2015). Seismic monitoring of an underground natural gas storage facility: The Collalto Seismic Network. *Seismological Research Letters*, *86*(1), 109–123. https://doi.org/10.1785/0220140087

Reggiani, P., & Sala, B. (1992). I mammut del Veneto. *Memorie di Scienze Geologiche*, *44*, 171–191.

Reiter, F., Freudenthaler, C., Hausmann, H., Ortner, H., Lenhardt, W., & Brandner, R. (2018). Active seismotectonic deformation in front of the Dolomites indenter, Eastern Alps. *Tectonics*, *37*(12), 4625–4654. https://doi.org/10.1029/2017tc004867

Roeder, D., & Lindsey, D. (1992). Barcis area (Veneto, Friuli, Slovenia): Architecture and geodynamics. *Nafta*, *43*, 509–548.

Romano, M. A., Peruzza, L., Garbin, M., Priolo, E., & Picotti, V. (2019). Microseismic portrait of the Montello thrust (Southeastern Alps, Italy) from a dense high-quality seismic network. *Seismological Research Letters*, *90*, 1502–1517. https://doi.org/10.1785/0220180387

Rossato, S., Carraro, A., Monegato, G., Mozzi, P., & Tateo, F. (2018). Glacial dynamics in pre-Alpine narrow valleys during the Last Glacial Maximum inferred by lowland fluvial records (northeast Italy). *Earth Surface Dynamics*, *6*(3), 809–828. https://doi.org/10.5194/esurf-6-809-2018

Rovida, A., Locati, M., Antonucci, A., & Camassi, R. (Eds.). (2017). *Archivio Storico Macrosismico Italiano (ASMI)*. Istituto Nazionale di Geofisica e Vulcanologia (INGV). https://doi.org/10.13127/asmi

Sacco, F. A. (1898). *Anfiteatri morenici del Veneto* (Vol. 41). Annali della R. Accademia di Agricoltura.

Schmid, S. M., Pfiffner, O. A., Froitzheim, N., Schönborn, G., & Kissling, E. (1996). Geophysical-geological transect and tectonic evolution of the Swiss-Italian Alps. *Tectonics*, *15*(5), 1036–1064. https://doi.org/10.1029/96tc00433

Schoell, M. (1980). The hydrogen and carbon isotopic composition of methane from natural gases of various origins. *Geochimica et Cosmochimica Acta*, *44*(5), 649–661. https://doi.org/10.1016/0016-7037(80)90155-6

Schoell, M. (1988). Multiple origins of methane in the Earth. *Chemical Geology*, *71*(1–3), 1–10. https://doi.org/10.1016/0009-2541(88)90101-5

Schönborn, G. (1999). Balancing cross-sections with kinematic constraints: The Dolomites (northern Italy). *Tectonics*, *18*(3), 527–545. https://doi.org/10.1029/1998TC900018

Selli, L. (1998). Il Lineamento della Valsugana fra Trento e Cima d'Asta: Cinematica neogenica ed eredità strutturali permo-mesozoiche nel quadro evolutivo del Sudalpino Orientale (NE-Italia). *Memorie della Societa Geologica Italiana*, *53*, 503–541.

Serpelloni, E., Vannucci, G., Anderlini, L., & Bennett, R. A. (2016). Kinematics, seismotectonics, and seismic potential of the eastern sector of the European Alps from GPS and seismic deformation data. *Tectonophysics*, *688*, 157–181. https://doi.org/10.1016/j.tecto.2016.09.026

Sibson, R. H. (1995). Selective fault reactivation during basin inversion: Potential for fluid redistribution through fault-valve action. *Geological Society, London, Special Publications*, *88*(1), 3–19. https://doi.org/10.1144/gsl.sp.1995.088.01.02

Sinclair, H. D. (1997). Tectonostratigraphic model for underfilled peripheral foreland basins: An alpine perspective. *Bulletin of the Geological Society of America*, *109*(3), 324–346. https://doi.org/10.1130/0016-7606(1997)109<0324:tmfupf>2.3.co;2

Slejko, D., Rebez, A., & Santulin, M. (2008). Seismic hazard estimates for the Vittorio Veneto broader area (N.E. Italy). *Bollettino di Geofisica Teorica ed Applicata*, *49*, 329–356.

Sommaruga, A. (1999). Décollement tectonics in the Jura foreland fold-and-thrust belt. *Marine and Petroleum Geology*, *16*(2), 111–134. https://doi.org/10.1016/s0264-8172(98)00068-3

Stefani, C., Fellin, M. G., Zattin, M., Zuffa, G. G., Dalmonte, C., Mancin, N., & Zanferrari, A. (2007). Provenance and paleogeographic evolution in a multi-source foreland: The Cenozoic Venetian-Friulian Basin (NE Italy). *Journal of Sedimentary Research*, *77*(11), 867–887. https://doi.org/10.2110/jsr.2007.083

Stuart, A. J. (2005). The extinction of woolly mammoth (*Mammuthus primigenius*) and straight-tusked elephant (*Paleoloxodon antiquus*) in Europe. *Quaternary International*, *126*, 171–177. https://doi.org/10.1016/j.quaint.2004.04.021

Stuart, A. J., Sulerzhitsky, L. D., Orlova, L. A., Kuzmin, Y. V., & Lister, A. M. (2002). The latest woolly mammoths (*Mammuthus primigenius* Blumenbach) in Europe and Asia: A review of the current evidence. *Quaternary Science Reviews*, *21*(14–15), 1559–1569. https://doi.org/10.1016/s0277-3791(02)00026-4

Sugan, M., & Peruzza, L. (2011). Distretti sismici del Veneto. *Bollettino di Geofisica Teorica e Applicata*, *42*(Supplement), 3–90.

Trippetta, F., Petricca, P., Billi, A., Collettini, C., Cuffaro, M., Lombardi, A. M., et al. (2019). From mapped faults to fault-length earthquake magnitude (FLEM): A test on Italy with methodological implications. *Solid Earth*, *10*(5), 1555–1579. https://doi.org/10.5194/se-10-1555-2019

Van Husen, D. I. R. K. (2000). Geological processes during the quaternary. *Mitteilungen der Osterreichischen Geologischen Gesellschaft*, *92*(1999), 135–156.

Vann, I. R., Graham, R. H., & Hayward, A. B. (1986). The structure of mountain fronts. *Journal of Structural Geology*, *8*(3–4), 215–227. https://doi.org/10.1016/0191-8141(86)90044-1

Venzo, S., with collaboration of Petrucci, F., & Carraro, F. (1977). I depositi quaternari e del Neogene Superiore nella bassa valle del Piave da Quero al Montello e del Paleopiave nella valle del Soligo (Treviso). *Memorie degli Istituti di Geologia e Mineralogia dell'Universita di Padova*, *30*, 1–27.

Verwater, V. F., Le Breton, E., Handy, M. R., Picotti, V., Jozi Najafabadi, A., & Haberland, C. (2021). Neogene kinematics of the Giudicarie Belt and eastern Southern Alpine orogenic front (northern Italy). *Solid Earth*, *12*(6), 1309–1334. https://doi.org/10.5194/se-12-1309-2021

ViDEPI. (2010). ProgettoViDEPI-visibilità dati esplorazione petrolifera in Italia. © 2009-2022-Ministero dello Sviluppo Economico UNMIG-Soc. Geol. It.-Assomineraria. On-line database Retrieved from www.videpi.com

Villa, A., Blain, H.-A., & Delfino, M. (2018). The Early Pleistocene herpetofauna of Rivoli Veronese (northern Italy) as evidence for humid and forested glacial phases in the Gelasian of Southern Alps. *Paleogeography, Paleoclimatology, Paleoecology*, *490*, 393–403. https://doi.org/10.1016/j.palaeo.2017.11.016

Von Hagke, C., & Malz, A. (2018). Triangle zones—Geometry, kinematics, mechanics, and the need for appreciation of uncertainties. *Earth-Science Reviews*, *177*, 24–42. https://doi.org/10.1016/j.earscirev.2017.11.003

Wegmann, K. W., & Pazzaglia, F. J. (2009). Late Quaternary fluvial terraces of the Romagna and Marche Apennines, Italy: Climatic, lithologic, and tectonic controls on terrace genesis in an active orogen. *Quaternary Science Reviews*, *28*(1–2), 137–165. https://doi.org/10.1016/j.quascirev.2008.10.006

Wells, D. L., & Coppersmith, K. J. (1994). New empirical relationships among magnitude, rupture length, rupture width, rupture area, and surface displacement. *Bulletin of the Seismological Society of America*, *84*(4), 974–1002.

Willett, S. D., Schlunegger, F., & Picotti, V. (2006). Messinian climate change and erosional destruction of the central European Alps. *Geology*, *34*(8), 613–616. https://doi.org/10.1130/g22280.1

Winterberg, S., Picotti, V., & Willett, S. D. (2020). Messinian or Pleistocene valley incision within the Southern Alps. *Swiss Journal of Geosciences*, *113*(1), 1–14. https://doi.org/10.1186/s00015-020-00361-7